OULUN YLIOPISTO
UNIVERSITY of OULU

DEGREE PROGRAMME IN WIRELESS COMMUNICATIONS ENGINEERING

MASTER'S THESIS

PAPR AWARE POWER ALLOCATION FOR OFDMA UPLINK

Author	Kushal Tiwari
Supervisor	Docent Antti Tölli
Second Examiner	Prof. Markku Juntti
Technical advisor	Dr. Valtteri Tervo

May 2015

Tiwari K. (2015) PAPR aware Power Allocation in OFDMA Uplink. University of Oulu, Department of Communications Engineering, Master's Degree Programme in Wireless Communications Engineering, 72 p.

ABSTRACT

This thesis investigates the power allocation scheme and essential design constraints to be considered in multicarrier systems particularly in the case of orthogonal frequency division multiple access (OFDMA) system in multiuser (MU) scenario. The compatibility between multicarrier system and multiple input multiple output (MIMO) system is exploited in designing the power allocation algorithm for a cellular network with multiusers. The multicarrier MIMO system facilitates dynamic resource allocation due to the decomposition of physical resources into multiple domains. The energy efficiency and interference management are the crucial aspects especially in uplink (UL) transmission. Limiting the power consumption of mobile terminals (MT) in uplink (UL) is inevitable due to the limited amount of available energy. Furthermore, the traditional multicarrier system introduces a dynamic peak power variation with respect to average power causing erroneous circuit behavior. This phenomenon is usually quantified as peak to average power ratio (PAPR). High PAPR drives the high power amplifier (HPA) into non-linear region to result in significant degradation in the system performance in terms of power efficiency. In this thesis an iterative power allocation algorithm is proposed to minimize the sum power and PAPR.

This thesis presents the power allocation strategy such that the PAPR is controlled during the power allocation (minimization) stage in frequency domain. The optimal power allocation is achieved by joint optimization of transmit power and receive beamformers (TX-RX) using convex optimization technique. The original problem is not jointly convex with respect to TX-RX. Therefore an iterative algorithm is proposed to optimize TX and RX alternatingly such that by calculating TX for given fixed set of RX and vice versa until convergence. The statistical approach is adopted to reduce the PAPR by actually minimizing the signal power variance (SPV) due to the fact that the large number of independent and identically distributed complex OFDMA symbols tends to follow Gaussian probability density function characterized by certain mean and variance. The non-convex constraints in the formulation are transformed into convex form using the successive convex approximation (SCA) with required change of variable (COV). The algorithm guarantees to maintain the user-specific quality of service (QoS) defined by the rate constraint.

Hence, equipped with the potentials of future generation technologies and using convex optimization as a tool, this thesis offers a sum power and PAPR minimization scheme for MU SIMO-OFDMA UL transmission.

Keywords: OFDMA, power minimization, PAPR reduction, MMSE

CONTENTS

ABSTRACT
CONTENTS
PREFACE

LIST OF SYMBOLS AND ABBREVIATIONS 5
1. INTRODUCTION 10
2. MULTICARRIER MODULATION AND OFDMA CONCEPT 13
2.1. Introduction to Multicarrier Communication 13
2.2. Orthogonal Frequency Division Multiplexing 15
2.2.1. Orthogonality using DFT 16
2.2.2. Cyclic Prefix 18
2.2.3. Drawbacks of orthogonal frequency division multiplexing (OFDM) system 20
2.2.3.1. Synchronization 20
2.2.3.2. Peak to average power ratio 22
2.3. SIMO-OFDM 29
2.4. Adaptive Power Allocation in OFDMA 29
2.5. Power Minimization Problem 32
2.6. Multiple Access with orthogonal frequency division multiple access (OFDMA) 34
2.7. OFDMA and SC-FDMA 35
3. SYSTEM MODEL AND SIMULATION SETUP 38
3.1. System Model 38
3.1.1. Transmitter 38
3.1.2. Receiver 41
3.2. MMSE-FDE Detection 43
3.3. SINR 45
3.4. Capacity 46
3.5. PAPR 46
4. PROBLEM FORMULATION AND OPTIMIZATION 47
4.1. Joint Power Allocation and Beamforming Problem with SINR and Rate constraint 47
4.1.1. Convexity 47
4.1.2. Log-Convex Transformation 48
4.2. PAPR aware Joint Power Allocation and Beamforming Problem with SINR and Rate constraint 50
4.2.1. Notion of multi-objective programming (MOP) and Pareto optimality 51
4.2.2. Solving PAPR Aware optimization problem 51
5. NUMERICAL ANALYSIS 54
6. DISCUSSION 62
BIBLIOGRAPHY 64
APPENDIX 68

PREFACE

This thesis work has been carried out in partial fulfilment of the requirements of the Master's Degree Programme in Wireless Communication Engineering at the Department of Communication Engineering, University of Oulu, Finland. The aim of this thesis is to study and formulate the power minimization problem for advanced wireless cellular systems. Working on this thesis has been challenging but at the same time it has also been highly educating. Hence, I would like to gratefully acknowledge the Centre for Wireless Communication (CWC), Department of Communications Engineering (DCE) and University of Oulu for this opportunity provided to me to conduct a research on this very important and pertinent subject and learn a lot on the subject through the valuable interactions with the distinguished faculty of DCE.

I would like to express my sincere gratitude to my supervisor Docent Antti T*ö*lli for giving me this opportunity to carry out the thesis work under his guidance. I am extremely grateful for his enduring support, guidance and encouragement to accomplish the assignment.

My deepest appreciation goes to Dr. Valtteri Tervo for his supervision, advice and his valuable and inspiring guidance throughout the duration of this thesis work. I would like to heartily thank him for his encouragement to tackle the difficult situations in the course of completion of this thesis.

Lastly my special thanks go to my parents and friends for their unconditional support and motivation throughout my thesis work.

LIST OF SYMBOLS AND ABBREVIATIONS

$\lvert \cdot \rvert$	absulte value operator
$\mathbf{A}\{\cdot\}$	autocorrelation operator
μ_P	average signal power
$\tilde{\mathbf{b}}_u$	estimate of baseband symbol vector b_u transmitted by user u ($N_F \times 1$)
$\tilde{b}_{u,k}$	estimate of baseband symbol $b_{u,k}$ transmitted at the k^{th} subcarrier of user u
$\mathbf{b}$	complex baseband datastream
$bdiag[\cdot]$	block diagonal operator
N_F	number of subcarriers
$c_{u,k}$	data rate achieved at the k^{th} subcarrier of user u
c_u	data rate achieved by user u
$\lambda^r_{u,k}$	channel frequency response for the k^{the} subcarrier of user u at receive antenna r
$\mathbf{\Gamma}_u$	space frequency channel matrix for the u^{th} user across N_R receive antennas ($N_R N_F \times N_F$)
$\mathbf{\Gamma}$	overall concatenated space frequency channel matrix for all the N_F subcarriers of all U users across N_R receive antennas ($N_R N_F \times U N_F$)
$\mathbf{\Gamma}^r_u$	space frequency diagonal channel matrix for the u^{th} user at receive antenna r ($N_F \times N_F$)
$\lambda_{u,k}$	channel frequency responses at the k^{the} subcarrier of user u across N_R receive antennas ($N_R \times 1$)
R_H	chi-squared distribution of a time domain samples of OFDM symbol
L	number of channel taps
χ	chi-squared distribution of a time domain samples of OFDM symbol
$h^r_{u,k}$	complex time domain fading coefficient for the k^{th} subcarrier of user u at receive antenna r
$\mathbf{H}_u$	space time circulant channel matrix for the u^{th} user across N_R receive antennas ($N_R N_F \times N_F$)
$\mathbf{H}^r_u$	space time circulant channel matrix for the u^{th} user at receive antenna r ($N_F \times N_F$)
$h^r_{u,l}$	complex time domain fading coefficient with respect to l^{th} path of user u for receive antenna r
$circ[\cdot]$	circulant operator
B_c	coherence bandwidth of channel
$(\cdot)^*$	complex conjugate
$\mathbb{C}$	complex number
$\mathbf{b}(t)$	continous complex baseband signal at time instant t
$\mathbf{h}(t)$	impulse response function of multipath wireless channel at time instant t
$\mathbf{s}(t)$	continous passband transmitted signal at time instant t
$\mathbf{r}_b(t)$	continous passband transmitted signal at time instant t
$\mathbf{r}(t)$	continous received signal at time instant t
$\star$	convolution operator
N_{CP}	length of cyclic prefix

T_d	delay spread
Δf	subcarrier frequency spacing
$f_{k,m}$	each element of DFT matrix F
$\mathbf{F}_{N_R}$	block diagonal matrix consisting of N_R blocks of DFT matrix F ($N_R N_F \times N_R N_F$)
$\mathbf{F}$	DFT matrix ($N_F \times N_F$)
$\tilde{\mathbf{n}}$	frequency response of additive white gaussian noise across N_R receive antennas ($N_R N_F \times 1$)
$g_{k,m}$	elements of matrix G
$\mathbf{G}$	matrix representing the matrix multiplication between DFT matrix and power allocation matrix ($N_F \times N_F$)
$\tilde{r}^r_{u,k}$	received sample of frequency domain OFDM symbol at the k^{th} subcarrier of user u at receive antenna r
$\tilde{\mathbf{r}}_u$	single user perspective representation of the received frequency domain OFDM symbol vector $\tilde{\mathbf{r}}$ ($N_R N_F \times 1$)
$\tilde{\mathbf{r}}$	received frequency domain OFDM symbol vector across N_R receive antennas ($N_R N_F \times 1$)
$\mathbf{P}_u$	power allocation matrix for u ($N_F \times N_F$)
$diag[\cdot]$	diagonal operator
N	effective length of OFDM after CP insertion
$\|\cdot\|$	Euclidean norm
$\mathbb{E}\{\cdot\}$	Expectation operator
$(\cdot)^H$	complex conjugate transpose (Hermitian)
$\mathbf{I}_N$	identity matrix ($N \times N$)
$P^0_{u,k}$	initial feasible power allocated to the k^{th} subcarrier of user u
$\hat{\gamma}^0_{u,k}$	initial feasible SINR for the k^{th} subcarrier of user u
$\hat{t}^0$	initial feasible signal power variance
$\otimes$	the Kronecker product
$\alpha_{u,k}$	representation of power ($P_{u,k}$) in logarithmic domain
t	representation of signal power variance ($\sigma^2_{P_u}$) in logarithmic domain
$\omega_{u,k}$	linear mmse estimator vector for k^{th} subcarriers of user u across N_R receive antennas ($N_R \times 1$)
$\omega^r_{u,k}$	mmse estimator for k^{th} subcarrier of user u at receive antenna r
$\mathbf{\Omega}^r_u$	mmse weight diagonal matrix for user u at receive antenna r ($N_F \times N_F$)
$\mathbf{\Omega}_u$	mmse weight matrix for user u across N_R receive antennas ($N_R N_F \times N_F$)
$\ln(\cdot)$	natural log operator
$P^*_{u,k}$	optimal power achieved for the k^{th} subcarrier of user u at a given iteration
$\hat{P}_{u,k}$	new updated power for the k^{th} subcarrier of user u to be used in next iteration
$\hat{\gamma}^*_{u,k}$	approximated feasible SINR for the k^{th} subcarrier of user u at a given iteration
$\hat{t}^*$	approximated feasible signal power variance at a given iteration
σ^2_n	noise power variance
$\mathbf{n}$	complex AWGN vector across N_R receive antennas ($N_R N_F \times 1$)
$\mathcal{CN}(\mu, \sigma)$	Circularly symmetric complex normal distribution with mean μ and variance σ

$\mathbf{\Psi}^k$	normalized channel gain matrix for the k^{th} subcarrier
ε	normalized carrier frequency offset
T_{ofdm}	OFDM symbol time period
Δf_o	carrier frequency offset
$\hat{\mathbf{p}}^k$	achievable optimal power vector for k^{th} subcarriers for U users($U \times 1$)
$\hat{\gamma}_{u,k}$	new updated SINR for the k^{th} subcarrier of user u to be used in next iteration
$\hat{t}$	new updated signal power variance to be used in next iteration
B	overall transmission bandwidth
δ_u	user specific PAPR of OFDM symbol
$\mathbf{b}_u$	complex baseband parallel data vector of user u ($N_F \times 1$)
$b_{u,k}$	complex baseband parallel data of user u at the k^{th} subcarrier
τ	delay associated with the multipath
ϕ	phase factor
$\mathbf{P}$	block diagonal power allocation matrix for U users ($UN_F \times UN_F$)
$P_{u,k}$	power allocated to bitstream at the k^{th} subcarrier of user u
$\mathbf{p}^k$	power vector for k^{th} subcarriers of U users ($U \times 1$)
$Pr(\cdot)$	probability
R_u	user specific rate constraint
$\mathbb{R}$	real number
$\mathbf{A}_{\tilde{r}\tilde{r}}$	autocorrelation matrix of received signal vector $\tilde{r}$ ($N_R N_F \tilde{N}_R N_F$)
$r^r_{u,k}$	received sample of time domain OFDM symbol at the k^{th} subcarrier of user u at receive antenna r
$\mathbf{r}_u$	single user perspective representation of the received time domain OFDM symbol vector $\mathbf{r}$ ($N_R N_F \times 1$)
$\mathbf{r}$	received time domain OFDM symbol vector across N_R receive antennas after CP removal ($N_R N_F \times 1$)
N_R	number of receive antennas
$\mathbf{A}_{\tilde{r}b_u}$	cross-correlation matrix between received signal vector $\tilde{r}$ and baseband symbol vector b_u of the u^{th} user ($N_R N_F \tilde{N}_F$)
$\mathbf{x}_u$	original complex serial data stream of user u
$\sigma^2_{P_u}$	normalized signal power variance for user U
$\gamma_{u,k}$	SINR of user u at the k^{th} subcarrier
γ_{min}	minimum fixed SINR threshold for each subcarrier
$\rho(\mathbf{\Psi}^k)$	spectral radius of normalized channel gain matrix for the k^{th} subcarrier
T_s	symbol duration
θ_i	scalar weight on the i^{th} objective term of optimization problem
$\mathbf{s}_u$	transmitted OFDM symbol vector of user u ($N_F \times 1$)
$s_{u,k}$	OFDM modulated time domain sample at the k^{th} subcarrier of user u
N_T	number of transmit antennas
U	number of users
3G	third Generation
3GPP	3rd Generation Partnership Project
4G	fourth Generation
ac	alternative current
ADC	analog to digital converter
AWGN	additive white gaussian noise

BC	broadcast channel
BER	bit error rate
BS	base station
CATV	community antenna television
CCDF	complementary cumulative distribution function
CDF	cumulative distribution function
CFR	channel frequency response
CIR	channel impulse response
COV	change of variables
CP	cyclic prefix
CSI	channel state information
CSIR	channel state information at the receiver
CSIT	channel state information at the transmitter
CV	coefficient of variation
DAC	digital to analog converter
DC	difference of convex
dc	direct current
DFT	discrete fourier transform
DL	downlink
DVB	digital video broadcasting
E-UTRA	Evolved Universal Terrestrial Radio Access
ETSI	European Telecommunications Standards Institute
FDE	frequency domain equalization
FDM	frequency division multiplexing
FFT	fast fourier transform
HPA	high power amplifier
i.i.d	independent, identically distributed
ICI	intercarrier interference
IDFT	inverse discrete fourier transform
IEEE	Institute of Electrical and Electronics Engineers
IMD	intermodulation distortion
IQ	in-phase and quadrature
ISI	intersymbol interference
LHS	left hand side
LMMSE	linear minimum mean square error
LMSC	LAN/MAN Standard Committee
LTE	Long Term Evolution
MAC	multiple access channel
MCM	multicarrier modulation
MIMO	multiple input multiple output
MISO	multiple input single output
MMSE	minimum mean square error
MMSE-FDE	minimum mean square error equalizer in frequency domain
MOP	multi-objective programming
MRC	maximal ratio combinig
MRT	maximal ratio transmission
MSE	mean square error
MT	mobile terminal
MU	multiuser

OFDM	orthogonal frequency division multiplexing
OFDMA	orthogonal frequency division multiple access
PA	power amplifier
PAPR	peak to average power ratio
PHY	physical layer
PTS	partial transmit sequence
QoS	quality of service
QPSK	quadrature phase shift keying
RF	radio frequency
RHS	right hand side
RRM	radio resource management
SC-FDE	single carrier frequency domain equalization
SC-FDMA	single carrier frequency division multiplexing access
SCA	successive convex approximation
SDP	semi-definite programming
SIMO	single input multiple output
SINR	signal to interference and noise ratio
SISO	single input single output
SLM	selected mapping
SNR	signal to noise ratio
SPV	signal power variance
SVD	singular value decomposition
TDM	time division multiplexing
TX-RX	transmit power and receive beamformers
UL	uplink
WiMAX	Worldwide Interoperability for Microwave Access
ZF	zero forcing

1. INTRODUCTION

The early discussions on the concept of parallel data transmission using OFDM [1] can be found in [2–4] dating back to 1957. It was only after 2001 when Institute of Electrical and Electronics Engineers (IEEE) 802 LAN/MAN Standard Committee (LMSC) introduced IEEE 802.16e standard [5] employing OFDMA. It gained popularity as a suitable physical layer (PHY) interface to achieve high speed data communication in the future generation of broadband wireless communications beyond third Generation (3G). The IEEE 802.16e standard also know as Worldwide Interoperability for Microwave Access (WiMAX) [6] paved a way towards developing a framework for fourth Generation (4G) network architecture. This led 3rd Generation Partnership Project (3GPP) to release their own OFDMA based communication system for 4G wireless communications standard also commonly known as Long Term Evolution (LTE) [7]. The main reason for OFDM technique to acquire fundamental level of appreciation is due to its ability to combat frequency-selective fading, improved spectral efficiency due to compact arrangement of orthogonal subcarriers and intersymbol interference (ISI) mitigation. OFDMA as a multiple access technique takes the inherited advantage from OFDM scheme and furthermore decomposes the physical channels which, at its lowest level are identified by the individual time frequency slot. The 4G PHY interface also enjoys the compatibility between OFDMA and multiple input multiple output (MIMO). Therefore the PHY interface technology of 4G system can precisely be called MIMO-OFDMA. The extension to spatial domain realized by MIMO introduces an additional dimension in the transmission resource such that each individual physical channel in MIMO-OFDMA system further decomposes to time frequency space slot. The benefits of MIMO-OFDMA system are increase in capacity, spectral efficiency, coverage and link reliability; however, each benefit is based on appropriate MIMO configuration [8–10] and involves certain trade-off among each other. With proper exploitation of the multiple diversities in various domains, the engineers are able to deign robust scheduling algorithms using advanced optimization techniques. Versatile algorithms designed for optimal resource utilization should be capable of fulfilling the user specific requirements depending on their transmission environment, with the general motive of enhancing the overall system performance.

While the multiple access technique adopted by WiMAX is OFDMA in both uplink (UL) and downlink (DL) channel, LTE uses separate schemes, particularly OFDMA in the DL channel and single carrier frequency division multiplexing access (SC-FDMA) in the UL channel. The choice of SC-FDMA reflects the vulnerability of UL channel towards the peak to average power ratio (PAPR). PAPR degrades the system performance in terms of power efficiency and battery operated devices like mobile terminal (MT) in UL are more susceptible to it. PAPR degrades the system performance of battery operated devices in terms of power efficiency. Reducing the PAPR in MIMO-OFDMA has been a subject of interest for many researchers due to its affect on performance of 4G systems [11–13]. Although the use of SC-FDMA reduces the PAPR, the system is deprived of many other advantages of OFDMA.

The 3GPP specification for 4G systems mentions power control with a great importance and considered as an integral part of the radio resource management (RRM). The power allocation in UL MIMO-OFDMA system is referred to as link adaptation due to the ability of each individual orthogonal subcarrier to adapt or modify itself as per demand on the basis of link quality. The efficient power allocation is important for following reasons:

- Energy conservation in case of battery powered device such as MT can be achieved by minimizing the power utilization. The aim is to allocate minimum power as possible, that is adequate to maintain certain quality of service (QoS). This also limits the total coverage of a MT.

- Power allocation is an elegant way to reduce the co-channel interference arising from other users in the same serving cell or neighbouring cells. Power minimization not only saves energy but also reduces interference. The 4G approach for interference mitigation is not to thrive on weak users by allocating them high power as it introduces high interference to other users. On the contrary, the strong users are highly favored due to their ability to achieve high performance even at low power.

The sum power and PAPR minimization algorithm in this thesis exercises the flexibility in scheduling offered by OFDMA system. This thesis aims to encourage useability of the OFDMA scheme in the UL scenario by making an attempt to reduce the PAPR at the power allocation stage. It has been shown in [14,15] that the power allocation in frequency domain (before inverse discrete fourier transform (IDFT) operation) creates high peaks in OFDM composite signal. This thesis presents the power allocation strategy such that the PAPR is controlled during the power allocation stage in frequency domain. Similar PAPR minimization technique has been presented in [16]. The thesis investigates a statistical approach of minimizing PAPR by reducing the signal power variance (SPV) of transmitted signal assuming that the samples in OFDM composite signal are normally distributed. This intuitive approach is preferred for the reason that both the parameters, namely PAPR and SPV are measure of dispersion around the average value. The problem formulation for sum power and PAPR minimization is modelled as an optimization problem with various inequality constraints. The optimization is performed in a centralized manner at the base station (BS) with the knowledge of full channel state information (CSI). The constraints maintain the user-specific QoS above the certain threshold. The QoS governs the optimal achievable system performance in terms of signal to interference and noise ratio (SINR) and SPV where both the quantities are function of power. The SINR is required to be high enough to maintain minimum data rate requirement while the SPV should be low enough to keep PAPR level as minimum as possible. The SINR function is jointly related to some of the most important parameters such as signal power, channel gain and interference, which governs the scheduling strategy in multiuser (MU) scenario.

The multi-objective problem is constructed as a linear combination of the sum power and SPV weighted by certain scalar values that governs the stress on particular objective for minimization. The optimal power allocation is achieved by joint optimization of transmit power and receive beamformers (TX-RX) using convex optimization technique. The original problem is not jointly convex with respect to TX-RX. Therefore an iterative algorithm is proposed to optimize TX and RX alternatingly such that by calculating TX for given fixed set of RX and vice versa until convergence. The power allocation problem for fixed RX still remains non-convex in the power domain. The formulation consists of non-convex interference coupled function such as SINR which is transformed into convex form such that the optimal solution relates to the original problem. The non-convex constraint is reformulated as difference of convex (DC) and transformed into convex form using the successive convex approximation (SCA) with required change of variables (COV). COV used to obtain log-convexity by transforming the variable to logarithmic domain and SCA is used to convexify the non-convex

constraints. At each optimization stage, SCA obtains a local solution by approximating the DC functions as a convex and requires number of iterations for convergence. Convex formulation and its corresponding iterative algorithm for joint TX-RX optimization problem are studied for three scenarios as i) sum power minimization with fixed minimum SINR constraint, ii) sum power minimization with SINR and minimum rate constraint and iii) relaxed multi-objective problem for minimizing sum power with additional SPV constraint.

2. MULTICARRIER MODULATION AND OFDMA CONCEPT

This chapter introduces the basic building blocks and working principle of MU SIMO-OFDMA model. It provides an insight regarding the choice of multicarrier modulation in new generation communication system. The individual characteristics of the OFDM and MIMO technique are presented with general equations. The SIMO-OFDMA model refers to the combination of these two technologies and the notion is further extended to multiuser scenario. The way of minimizing PAPR and transmit power in UL scenario during the resource allocation is discussed.

2.1. Introduction to Multicarrier Communication

This section outlines the basics of multicarrier modulation (MCM) and its implementation on development of OFDM systems. To illustrate the importance of multicarrier system it is worth mentioning the multipath propagation phenomenon of the wireless channel. Consider a complex baseband signal $b(t)$, where t is the time instant. The baseband passband representation is given by

$$s(t) = Re\{b(t)e^{i2\pi f_c t}\}, \tag{2.1}$$

where $s(t)$ is the passband signal to be transmitted at center frequency f_c. The signal $s(t)$ propagates through the wireless channel consisting of L multipath components defined by

$$h(t) = \sum_{m=1}^{L} \alpha_m \delta(t - \tau_m),$$

where $h(t)$ is the time domain impulse response function of multipath wireless channel, α_m is the channel impulse response (fading coefficient) for the m^{th} path and τ_m is the delay associated with the m^{th} path. The received signal $r(t)$ is given by convolution between transmitted signal $s(t)$ and channel impulse response $h(t)$ as

$$\begin{aligned} r(t) &= s(t) \star h(t) \\ &= Re\{\sum_{m=1}^{L} \alpha_m b(t - \tau_m) e^{(i2\pi f_c (t-\tau_m))}\} \\ &= Re\{\underbrace{[\sum_{m=1}^{L} \alpha_m b(t - \tau_m) e^{-(i2\pi f_c \tau_m)}]}\, e^{(i2\pi f_c t)}\}, \end{aligned}$$

where $\star$ is a convolution operator. The complex baseband received signal $r_b(t)$ can be represented as

$$r_b(t) = \sum_{m=1}^{L} \alpha_m b(t - \tau_m) e^{-(i2\pi f_c \tau_m)}, \tag{2.2}$$

where $e^{-(i2\pi f_c \tau_m)}$ denotes the complex phase factor arising due to the delay τ_m, α_m exhibits rayleigh distribution and τ_m exhibits uniform distribution. From (2.1) and (2.2), it is seen that transmitting a signal $b(t)$ through L path wireless channel, the received baseband signal $r_b(t)$ is a summation of L copies of the transmitted signal arriving through each path $m, m = 1, 2, \cdots, L$ and each copy is influenced by its own channel fading coefficient α_m and complex phase factor $e^{-(i2\pi f_c \tau_m)}$.

Therefore, multipath propagation results in various replicas of the transmitted signal arriving at the receiver via different paths. The different signals are received by virtue of having travelled different paths and each path is defined by the distance adapted with different amplitude and phase which at the receiver either adds up constructively or destructively in phase. This nature of the wireless propagation channel results in energy of transmitted symbol to spread beyond its time interval causing its energy to leak into succeeding symbol. This overlapping of symbols in time is known as ISI. The range of signal powers received at the receiver depends on the random fading coefficient of channel and this variation of the signal power at the receiver due to the random nature of multipath component is called *fading*. Furthermore, a deep fade may occur when combination of multiple copies of the signal at the receiver results in strong destructive interference such that the reliable signal detection is no longer possible. The channel's *delay spread* is a measure of propagation delay between the shortest and the longest multipath and *coherence bandwidth* of the channel is defined as inversely proportional to the delay spread. Coherence bandwidth is a channel bandwidth over which the frequency response is *flat*. Two types of fading effect due to multipath time delay spread are *flat fading* and *frequency selective fading*. Flat fading occurs when the bandwidth of the transmitted signal is less than the coherence bandwidth of the channel and can be represented as

$$B_c < B,$$

where B_c is the coherence bandwidth of the channel and B is the bandwidth of the communication system. The received signal can be analyzed as some scaled version of the narrowband transmitted signal passed through flat frequency response of the channel. This hugely reduces the equalization complexity at the receiver as the frequency response characteristics of the received signal is relatively flat or nearly equal. It also implies that the symbol period is much larger compared to the channel delay spread such that the time domain symbols do not overlap or each symbol overlaps with itself, thus ISI is eliminated.

On the other hand frequency-selective fading occurs when the bandwidth of the transmitted signal is more than the coherence bandwidth of the channel and can be represented as

$$B_c > B.$$

In the case of frequency selective channel, the transmitted signal is severely distorted causing ISI in time domain. As the wideband transmitted signal bandwidth is larger than the coherence bandwidth of the channel, the portion of the signal beyond the coherence bandwidth are highly attenuated and requires multiple tap equalization at the receiver.

Multicarrier modulation is a physical layer technique used to combat the hostile frequency selective fading encountered in wireless channel. The key contribution of multicarrier communication system is that it converts the wideband frequency selective channel into group of parallel narrowband flat fading channels which is a revolutionary

communication technology that forms the basis for 4G to achieve higher data rate. Therefore the MCM provides reliable detection at the receiver and mitigates the ISI in time domain. MCM utilizes the principle of transmitting data by decomposing the original data stream into several symbol streams having much lower symbol rate and each substream is used to modulate different subcarriers and transmitted separately.

Consider a spectrum with two sided bandwidth of width B. In single carrier scenario, B can be considered as the symbol rate. The MCM technique divides the entire system bandwidth B into multiple subcarriers. If N_F is the total number of subcarriers then the separation between each subcarrier will be $\Delta f = B/N_F$. Overall symbol rate of the multicarrier transmission system is given by $\frac{N_F}{(N_F/B)} = B$. It shows that the overall system capacity is invariant in MCM compared to that of singlecarrier as multicarrier transmits N_F symbols using N_F subcarriers in time period $T_{ofdm} = 1/\Delta f$ while single carrier transmits one symbol in time period $T_s = 1/B$ resulting net symbol rate to be B in the both cases. Therefore the motive behind implementing multicarrier technique, lies not in increasing the capacity of the system but to achieve high data rates as a result of its capability to overcome the challenges imposed by propagation mechanism of wireless channels by increasing the actual symbol duration N_F times. Fig. 2.1 shows the time-frequency relation between singlecarrier and multicarrier.

2.2. Orthogonal Frequency Division Multiplexing

In earlier MCM system employing time limited signals were difficult to realize because of tremendous complexity in implementing bank of N_F modulators and demodulators at the transmitter and receiver using analog subcarrier oscillators and filters which demands wider bandwidth. Therefore, the concept of OFDM was once abandoned due to difficulty in subcarrier recovery without inter-subcarrier interference until the development of concept of using discrete fourier transform (DFT) in MCM for time-limited orthogonal signals. Further the concept was reinforced by development of efficient DFT algorithm such as fast fourier transform (FFT) [17]. This system of transmission was named OFDM. OFDM is a modulation scheme suitable for new generation broadband communication systems that obeys the multicarrier modulation principle discussed in section 2.1. OFDM is an advanced form of frequency division multiplexing (FDM) built on basis of MCM principle. It divides the actual information data stream into parallel data symbols and transmit the symbols using multiple orthogonal subcarriers that shares the overall system bandwidth. In time limited OFDM signal, the spectra of subcarriers overlap with each other but the information being transmitted are still separated due to the orthogonality principle. The overlapping of the spectrum allows efficient utilization of the available system bandwidth.

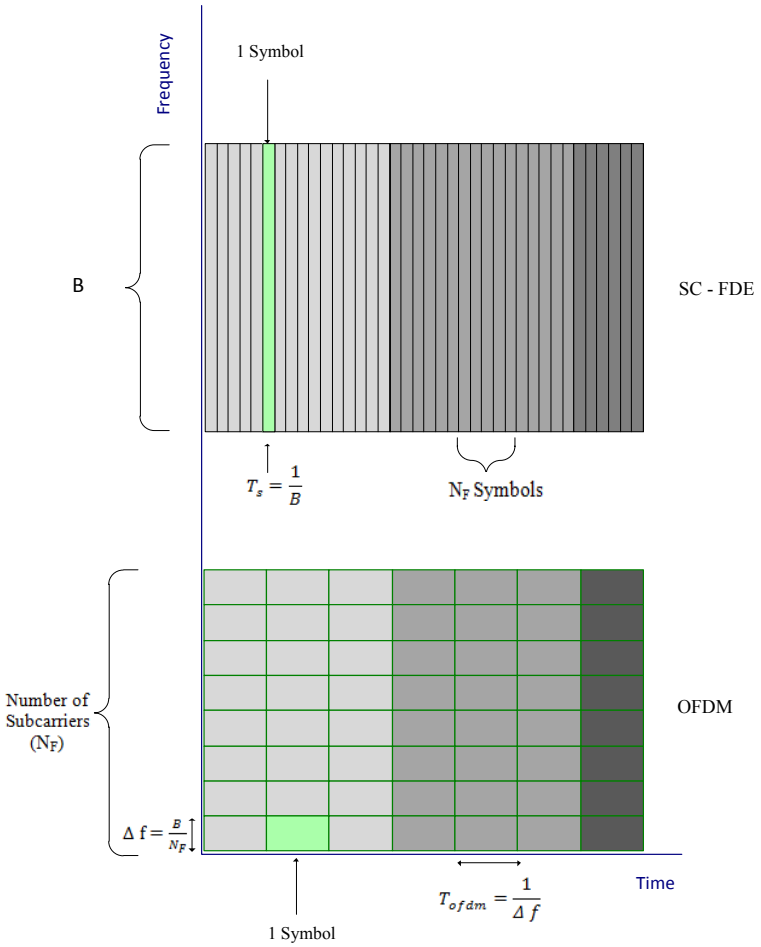

Figure 2.1: Singlecarrier vs Multicarrier.

2.2.1. Orthogonality using DFT

The DFT modulation implicitly spaces the subcarriers in such a way that at each frequency, where the received signal is evaluated all the other signals at different frequencies are zero. The orthogonality principle is essential for OFDM signal to eliminate intercarrier interference (ICI). In OFDM system the frequency domain signal refers to the parallel data stream before IDFT operation.

Consider a MCM system with N_f subcarriers i.e. the system transmits N_F parallel data stream simultaneously. The multicarrier composite transmit signal $s(t)$ at the time instant t is given by

$$s(t) = \sum_{m=1}^{N_F} b_m e^{(i2\pi(m-1)Bt/N_F)}, \tag{2.3}$$

where b_m is the frequency domain m^{th} complex data to be transmitted, $\Delta f = B/N_F$ denotes the subcarrier separation and $m(\Delta f)$ is the center frequency used to modulate m^{th} data. (2.3) shows that each low data rate $1/(N_F T_s)$ modulated signal sums up to

a high data rate transmission $1/T_s$.

Consider the k^{th} sample from the multicarrier symbol. The time instant t can be written as

$$t = kT_s, \quad k = 1, 2, \cdots, N_F$$

where $T_s = 1/B$ is the sample interval or a symbol duration. Then the signal s_k denoting the k^{th} sample of multicarrier transmission or equivalently the data transmitted on the k^{th} subcarrier can be expressed as

$$\begin{aligned} s_k = s(kT_s) &= \sum_{m=1}^{N_f} b_m e^{(i2\pi(m-1)(k-1)B/BN_F)} \\ &= \sum_{m=1}^{N_f} b_m e^{(i2\pi(m-1)(k-1)/N_F)} \quad k = 1, 2, \cdots, N_F. \end{aligned} \tag{2.4}$$

Right hand side (RHS) of (2.4) is the IDFT of the original information signal. Therefore the MCM composite transmit signal constitutes of samples generated by sampling at rate kT_s with help of IDFT operation. This scheme of generating composite transmit signal by employing IDFT was first proposed in [17]. The system implementing *MCM* technique by employing *IDFT* operation is termed as OFDM.

Orthogonality allows the subcarriers to overlap while eliminating crosstalk among each other. The orthogonality among the subcarriers depends on the choice of subcarrier separation Δf such that orthogonality in N_F equally spaced subcarriers can be achieved if

$$\Delta f = \tfrac{1}{N_F T_s} = \tfrac{1}{T_{ofdm}},$$

where T_{ofdm} is the total duration to transmit N_F symbols i.e. the overall OFDM symbol. Each element of the DFT matrix can be written as

$$f_{k,m} = \frac{1}{\sqrt{N_F}} e^{(i2\pi(m-1)(k-1)/N_F)} \quad m, k = 1, 2, \cdots, N_F, \tag{2.5}$$

where DFT coefficients follow the N_F^{th} roots of unity and $1/\sqrt{N_F}$ is a normalizing factor for N_F point DFT to maintain unity norm to prevent the norm of basis function to grow to $\sqrt{N_F}$. The result of IDFT, s_k in (2.4) is the *coefficient of projection* of the input vector $\mathbf{b}$ on the k^{th} DFT row vector f_k. If $\|\mathbf{f}_k = 1\|$, then

$$s_k = \langle \mathbf{b}, \mathbf{f}_k \rangle. \tag{2.6}$$

Projection preserves the orthogonality in frequency domain in such a way that the samples of overall spectrum of transmitted OFDM symbol taken at the spacing of $1/T_{ofdm}$ apart, represents the data modulated on each subcarrier and the samples are ICI free. The shape of subcarrier spectrum can be represented by $sinc(1/T_{ofdm})$, and sampling at the peak value of each spectrum $(kT_s),\ k = 1, 2, \cdots, N_F$ gives the $m^{th},\ m = 1, 2, \cdots, N_F$ baseband data and orthogonality ensures that at the sampling

point of the desired subcarrier k, all the other subcarriers $l \neq k,\ k, l = 1, 2, \cdots, N_F$ are null. Mathematically orthogonality of two complex exponential signals $s_k(n)$ and $s_l(n)$ can be represented as

$$\langle s_k, s_l \rangle = \sum_{n=0}^{N_F-1} s_k(n) s_l^*(n) \tag{2.7}$$

$$= \sum_{n=0}^{N_F-1} e^{(i2\pi nk/N_F)} e^{-(i2\pi nl/N_F)} \tag{2.8}$$

$$= \sum_{n=0}^{N_F-1} e^{(i2\pi n/N_F)(k-l)} \tag{2.9}$$

$$= \frac{1 - e^{(i2\pi(k-l))}}{1 - e^{(i2\pi(k-l)/N_F)}}, \tag{2.10}$$

where $*$ denotes complex conjugate. If $k \neq l$, then the signals $s_k(n)$ and $s_l(n)$ are orthogonal to each other. Therefore,

$$\langle s_k, s_l \rangle = 0 \quad \Rightarrow s_k \perp s_l, \quad k \neq l.$$

The DFT matrix is used to decompose or convert the wideband frequency-selective channel into parallel narrowband flat-fading channels at the receiver. Each frequency domain input data at the receiver can be represented as some scaled version of the transmitted signal where scaling factors are equal to flat-fading channel frequency responses determined from the channel decomposition. The receiver utilizes the unique spatial signature (channel frequency response (CFR)) corresponding to each flat fading narrowband channel to estimate the original data. This allows the use of frequency domain equalization (FDE) to obtain the receive beamformers in ISI free environment with reduced receiver complexity.

2.2.2. Cyclic Prefix

Cyclic prefix (CP) in OFDM system is a technique of increasing the OFDM symbol duration to mitigate the ISI resulting from time dispersion caused by multipath propagation [18]. Cyclic prefix also known as the guard interval works on the basis of DFT property along with the convolution theorem. The circular convolution between two time domain functions is equivalent to multiplication of their respective DFT's. In the real wireless environment the transmitted OFDM signal convolves linearly with the channel impulse response in time domain. After the CP extension of OFDM symbol, the linear convolution between the transmitted symbol and the channel impulse response yields the same result as that of circular convolution. This helps in decoupling the channel in frequency domain such that channel frequency response for each subcarrier is independent which is equivalent to converting the wideband frequency selective channel into group of N_F parallel narrowband flat fading channel. In general, the per subcarrier decoupling of the frequency domain received signal in OFDM system can be represented as

$$\tilde{r}_k = \lambda_k b_k + \tilde{n}_k \qquad k = 1, 2, \cdots, N_F,$$

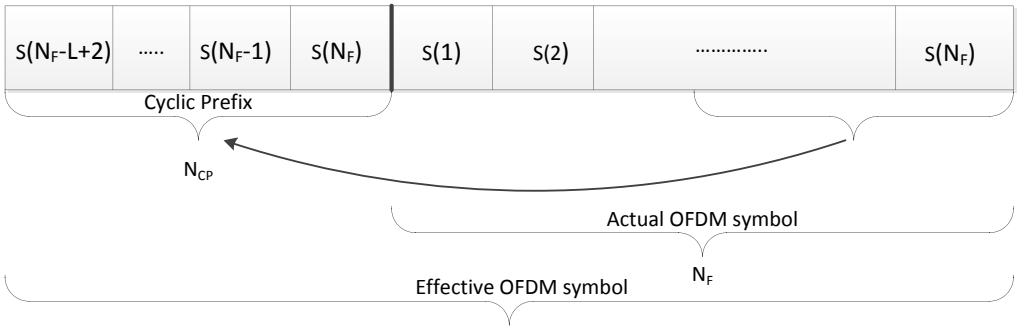

Figure 2.2: Cyclic prefix extended OFDM symbol.

where $\tilde{r}_k$ is the frequency domain received signal at the k^{th} subcarrier, λ_k is the channel frequency response associated with k^{th} subcarrier, b_k is the data transmitted on k^{th} subcarrier and $\tilde{n}_k$ is zero mean, unit variance additive white gaussian noise in frequency domain.

The technique significantly reduces the complexity in receiver design by employing FDE. Implementing cyclic prefix requires the knowledge of multipath characteristics of the channel, which governs the length of the cyclic prefix. The duration of the cyclic prefix length N_{CP} is chosen to be longer than the delay spread of the channel given by

$$N_{CP} \times T_s \geq T_d \,,$$

where N_{CP} is the cyclic prefix length, T_s is the symbol duration and T_d is the delay spread. Now the effective length of the extended OFDM symbol becomes $N = N_F + N_{CP}$ increasing the overall symbol duration of the effective OFDM symbol. The cyclic prefix takes N_{CP} samples from the end of a single OFDM symbol and pastes it in front of it as shown in the Fig. 2.2. The concatenation of actual OFDM symbol with the CP increases the symbol duration of the effective OFDM symbol and also maintains the periodicity of the time domain OFDM symbol. Therefore the benefits of CP in OFDM symbol is as follows.

- Cyclic prefix acts as a guard interval between two adjacent symbols by preventing the arrival of a symbol at the receiver until all the multipath components of the previous symbol have arrived. Increase in symbol duration ensures that the delayed component from previous symbol do not interfere with the current symbol. Hence, no adjacent symbols overlap during the actual OFDM symbol window of length N_F.

- The periodicity achieved by CP prevents the impact of phase discontinuity during the superposition of its multi path components. The periodicity preserves the cyclic property of DFT by limiting the signal distortion to occur outside of the actual OFDM symbol. Therefore no phase transition occurs inside the actual OFDM window and the signal inside this observation window is formed by overlapping of phase shifted pure sinusoids. The frequency domain components in the actual OFDM symbol will contain an integer number of cycles corresponding to its subcarrier frequency. This is important for DFT to accurately identify every individual frequency components in the received time domain signal. The possibility of accurate identification of each frequency component in the received

signal allows the decoupling of channel in frequency domain. The transmitted OFDM symbol are sometimes oversampled by introducing zero padding to increase the accuracy of DFT. Although overlap between multiple copies of same symbol results in phase shift, ISI will be eliminated and orthogonality is maintained among the subcarriers.

The additional repeated samples decrease the spectral efficiency leading to loss in throughput of the system. The loss in efficiency due to cyclic prefix is given by N_{CP}/N. Hence as the number of subcarrier N_F increases, smaller portion of the symbol is affected by ISI but in turn also increases the processing time at the receiver. The optimal CP length to mitigate ISI by increasing the OFDM symbol duration N_F/B must satisfy the given condition

$$B_c \geq \frac{B}{N_F},$$

where B_c is the coherence bandwidth of the channel and B/N_F is the subcarrier bandwidth. The implementation of cyclic prefix is explained in Chapter 3.

2.2.3. Drawbacks of OFDM system

2.2.3.1. Synchronization

Due to the fact that the performance of OFDM system highly depends on orthogonality among subcarriers, it is more vulnerable to synchronization errors. Although OFDM systems increases spectral efficiency due to the overlapping subcarriers, even a small mismatch in the time or frequency synchronization can result in *loss of orthogonality* amongst subcarriers. Coherent detection at the receiver utilizes local oscillator (LO) to generate a signal with accurate carrier frequency and phase to recover the transmitted signal. The synchronization error during detection may arise due to various reasons such as LO instability, delay spread and doppler shift which leads to carrier frequency offset, carrier phase offset, in-phase and quadrature (IQ) imbalance and mismatch in timing reference. All these phenomena affects the system performance by inducing ICI and eventually degrading the signal to noise ratio (SNR).

Timing synchronization refers to identifying the starting point for detection of OFDM symbols at the receiver. Several algorithms have been developed for timing alignment that exploits the sample repetition in an OFDM symbol due to CP insertion. If CP duration is larger than the delay spread of the channel such that each OFDM symbol is ISI free, then a linear phase shift occurs at the output of the DFT due to the delay spread of multipath propagation channel. The mismatch can be detected and rectified during the reception of CP and further the result can be used in channel estimation. On the other hand, if CP duration is not long enough, then the ISI induced received OFDM symbol suffers distortion in both phase and amplitude [19]. Timing errors can be eliminated by choosing appropriate CP length.

Carrier frequency offset and phase offset in OFDM system can cause severe distortion with significant reduction in SNR. In presence of frequency offset, the sampling point of the received signal is changed such that orthogonality amongst subcarrier is violated as shown in the Fig. 2.3. The new sampling point of the desired subcarrier's signal is deviated from its peak value and further includes samples from adjacent subcarriers due to ICI. This results in attenuation and phase shift. The deviation from

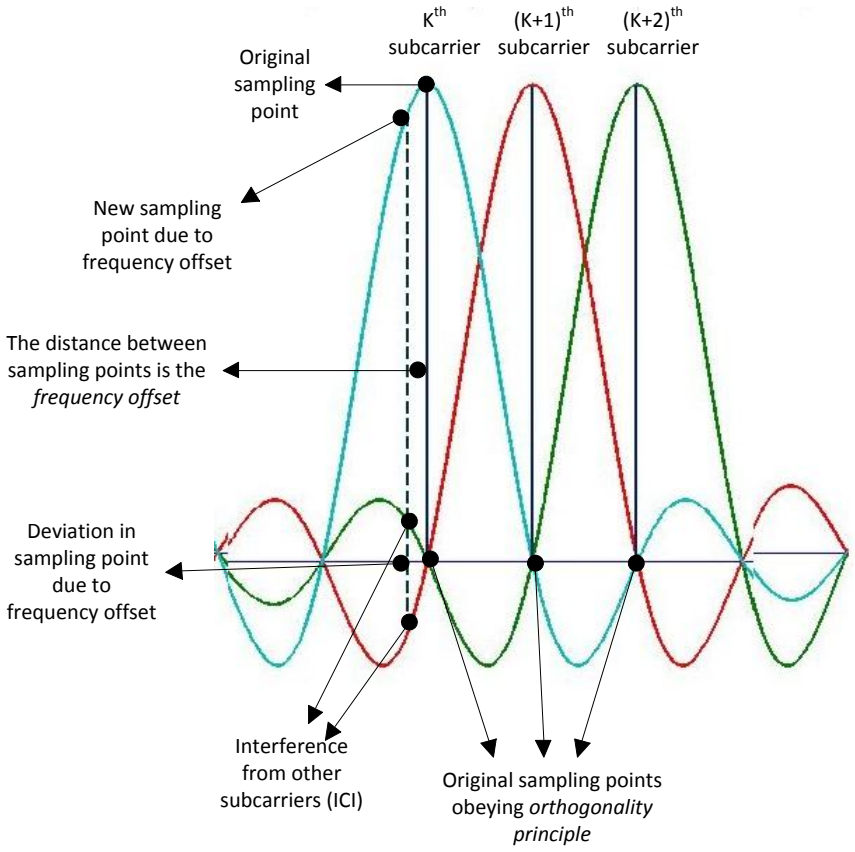

Figure 2.3: Carrier frequency offset.

peak value of the desired subcarrier signal results in loss of power and hence, degrades SNR.

Consider a frequency offset Δf_o. The normalized frequency offset ε with respect to subcarrier spacing is given by

$$\frac{\Delta f_o}{B/N_F} = \varepsilon,$$

In presence of normalized frequency offset ε, the frequency domain received signal across the k^{th} subcarrier can be represented as

$$\tilde{r}_k = \underbrace{\lambda_k b_k \frac{sin\pi\varepsilon}{sin\frac{\pi\varepsilon}{N_F}} \frac{1}{N_F} e^{i\tilde{\phi}_l}}_{\text{Desired Signal}} + \underbrace{\sum_{\substack{l=1 \\ l\neq k}}^{N_F} \lambda_l b_l \frac{sin\pi\varepsilon}{sin\pi\frac{l-k+\varepsilon}{N_F}} \frac{1}{N_F} e^{i\tilde{\phi}_{lk}}}_{\text{ICI}} + \tilde{n}_k, \tag{2.11}$$

where $\tilde{\phi}$ is the phase factor. The second term in (2.11) represents the ICI from the adjacent subcarriers. If the subcarriers are perfectly orthogonal to each other, then the second term will always be zero. The system model considered in this thesis assumes perfect synchronization with no carrier frequency offset.

2.2.3.2. Peak to average power ratio

PAPR in OFDM

PAPR is a critical limiting factor in OFDM modulation and degrades the performance of OFDM systems. The concept of PAPR arises from the fact that in OFDM systems instead of transmitting the original data symbols, the IDFT of these symbols are transmitted. IDFT preprocessing of N_F symbols causes superposition of N_F sine waves of random amplitudes and phases. Therefore summing up the IDFT of data symbols can produce high peaks for some combinations of sinusoids. This characteristics of IDFT causes significant *fluctuation* or *variation* in the instantaneous signal power (peak power) in composite signal with respect to it's average (mean) power.

The PAPR affects the performance of power amplifier (PA) used in the communication devices. The PA characteristics at the receiver can be analyzed in Fig. 2.4.

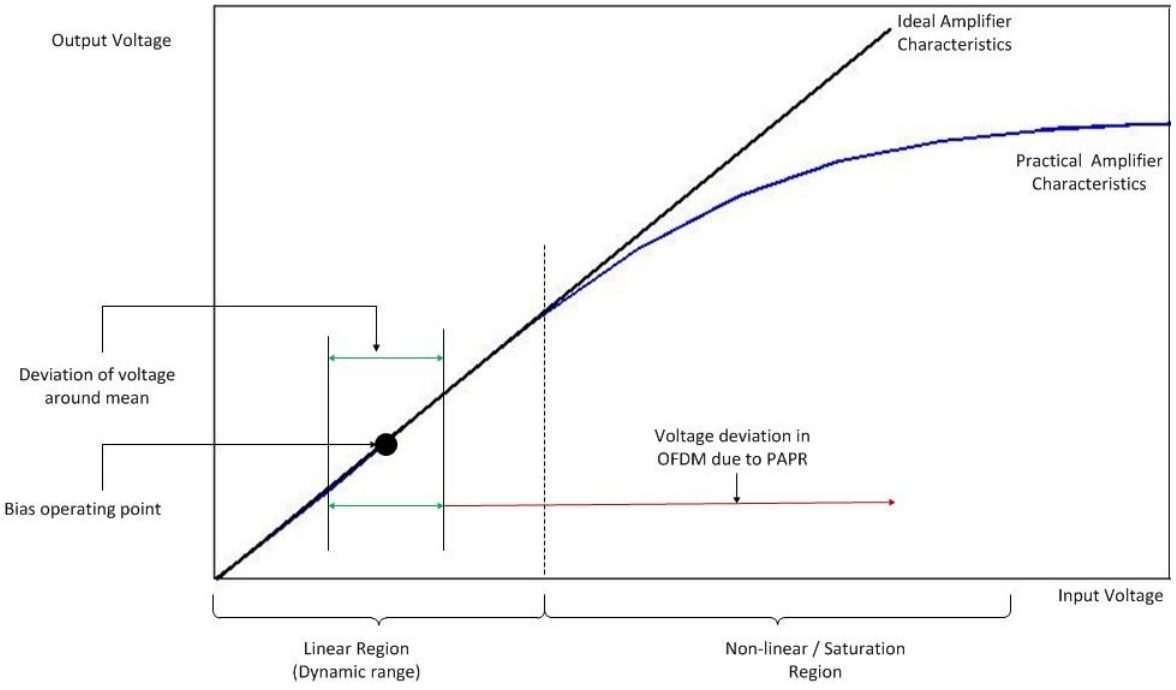

Figure 2.4: Power Amplifier characteristics.

The PA used at the transmitting end are high power amplifier (HPA) with capability of handling large-signals to provide sufficient power for transmission through an antenna so that the information in the received signal can be extracted with minimum distortion. PA is mainly characterized by its efficiency i.e. the maximum power that the amplifier circuit can handle. The operating point of a PA set by direct current (dc) bias is the region of operation of the amplifier and governs the alternative current (ac) response of the system. Ideally the operating point of the amplifier is chosen at the midpoint of the linear region to deal with maximum voltage or current swing. The ideal characteristic of PA in Fig. 2.4 is the linear region of its operation where the

output voltage is always some scaled version of the input signal. An ac signal at the amplifier input tends to vary the bias point from its established dc bias operating point. The larger the ac input, the higher the deviation across dc bias point causing swing in output voltage and current, driving the amplifier into non-linear region due to its saturation characteristics. Towards saturation, the output power of the PA is compressed with increasing input power. This phenomena affects the amplitude modulated signal by clipping off the peak values containing the information and causing rotation in phase modulated signal. Here the choice of operating point plays an important role in maintaining linearity, minimizing the distortion at the amplifier output and maximizing its dynamic range of amplification. A PA designed for OFDM signals needs to handle the occurrence of random high peaks such that the voltage and current swing at the output of the amplifier is restricted to dynamic range (linear region) or in other words the PA needs to utilize some *power backoff* scheme depending on the modulation used. Increasing power backoff scheme widens the dynamic range of PA but at the cost of reduced power efficiency. Low power efficiency leads to high power consumption. Therefore minimizing PAPR in UL OFDM system is crucial due to mobile terminals operating on limited battery power. The PA can be operated near the saturation region to increase the power efficiency. Failure to deal with high PAPR problem may drive PA into saturation resulting in ICI due to loss of orthogonality. The nonlinearity in PA also produces out of band distortion causing energy to spread across adjacent channels and in-band distortion affecting the signal constellation. Out of band distortion are caused by unwanted spurious responses and intermodulation distortion (IMD) products whose power increases at higher rate than the desired signal in the non-linear region. Apart from PA, the high PAPR also affects the dynamic margins of analog to digital converter (ADC) and digital to analog converter (DAC). The converters need high dynamic range to accommodate additional quantification levels to deal with the random occurring high peaks, thus degrading the SNR of the system by increase in quantification noise.

The PAPR of complex OFDM baseband signal can be defined as the ratio of the peak power to its average power. Using (2.5) the sample s_k allocated to the k^{th} subcarrier of the OFDM symbol can be represented as

$$\begin{aligned} s_k &= \frac{1}{\sqrt{N_F}} \sum_{m=1}^{N_F} b_m e^{(i2\pi(m-1)(k-1)/N_F)} \quad k = 1, 2, \cdots, N_F \\ &= \sum_{m=1}^{N_F} b_m f_{k,m} \quad k = 1, 2, \cdots, N_F, \end{aligned} \tag{2.12}$$

where $\frac{1}{\sqrt{N_F}}$ is the normalizing factor, b_m is the complex quadrature phase shift keying (QPSK) baseband data assumed to be statistically independent, identically distributed (i.i.d) random variables with zero mean, variance equal to $\mathbb{E}\{|b_m|^2\}$ and $f_{k,m}$ is the k, m element of DFT matrix.

The peak power is chosen among the complex baseband OFDM signal with maximum amplitude as

$$\max_{k\in[1,N_F]}|s_k|^2 = \max|\sum_{m=1}^{N_F} b_m f_{k,m}|^2$$
$$= \sum_{m=1}^{N_F}|b_m|^2$$

$$\max_{k\in[1,N_F]}|s_k|^2 = N_F|b_m|^2. \tag{2.13}$$

The average power of an composite OFDM signal is given by

$$\begin{aligned}\mathbb{E}\{|s_k|^2\} &= \frac{1}{N_F}\sum_{m=1}^{N_F}(\mathbb{E}\{|b_m|^2\}\mathbb{E}\{|f_{k,m}|^2\}) \\ &= \frac{1}{N_F}\sum_{m=1}^{N_F}\mathbb{E}\{|b_m|^2\} \\ &= \mathbb{E}\{|b_m|^2\},\end{aligned} \tag{2.14}$$

where $\mathbb{E}\{\cdot\}$ is the expectation operator. As per definition, the PAPR of single OFDM block is given by

$$\delta = \frac{\max_{k\in[1,N_F]}(|s_k|^2)}{\mathbb{E}\{|s_k|^2\}} = N_F\frac{|b_m|^2}{\mathbb{E}\{|b_m|^2\}}. \tag{2.15}$$

Highest peak occurs in OFDM symbol when all the subcarriers have identical phase and can be referred as the worst case PAPR scenario. According to (2.15), the PAPR increases linearly with the number of subcarriers. Hence, the HPA must be capable of handling the peak powers equal to N_F times the average power. The portion of cyclic prefix is not considered as it does not affect the overall peak or the average power of the OFDM symbol. However, it has been shown in [20] that the occurrence of high PAPR is not frequent.

Statistical distribution of PAPR

For more fair characterization of PAPR, the statistical distribution of the complex baseband OFDM samples are analyzed. The statistical analysis refers to measure of probability that the PAPR remains below specified critical value and desired confidence level can be achieved by performing analysis on all possible OFDM symbols. Consider QPSK modulated symbols denoted by b_m as shown in Fig. 2.5.

Each b_m symbol on IQ constellation is identified by its corresponding amplitude and phase. The OFDM subcarriers are created by modulating each of these symbols with frequency spacing of Δf such that each subcarrier are sinusoidals of integer number of cycles. The OFDMA system transmits each of these symbols in parallel over the symbol duration T_{ofdm}. The continuous time domain composite OFDMA signal s_t to

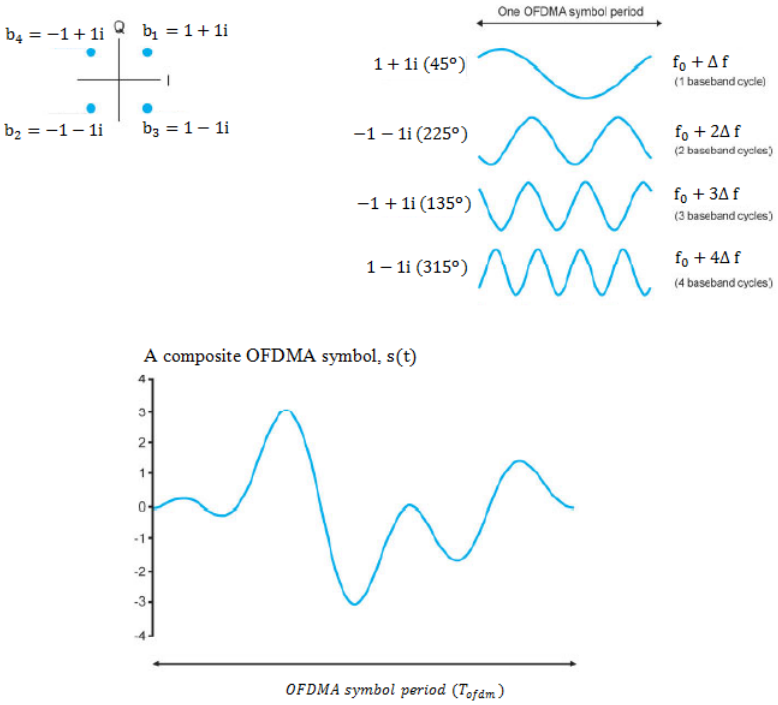

Figure 2.5: OFDM symbol as gaussian [21].

be transmitted is formed by summing up all the individual subcarriers. The increased peak value in the waveform of $s(t)$ compared to peak value of individual subcarrier is the resulting PAPR. Consider a single discrete complex baseband OFDMA symbol s_k in (2.12) formed by sampling the signal s_t of duration T_{ofdm} at the sampling rate of T_s. Generally, $m, k = 1, 2, \cdots, N_F$. Each sample in the sampling distribution s_k represents the summation of N_F different sinusoidals. Therefore for large number of N_F, the distribution of time domain OFDMA symbols across entire channel bandwidth B exhibits the normal (gaussian) characteristics in terms of PAPR. Complex valued s_k can be represented in cartesian coordinate and polar coordinate form as

$$s_k = \underbrace{x_k + iy_k}_{\text{Cartesian Form}} = \underbrace{a_k e^{i\phi_k}}_{\text{Polar Form}},$$

where the absolute value $a_k = |s_k| = \sqrt{x_k^2 + y_k^2}$ is the amplitude of the k^{th} sample of complex baseband OFDM symbol and $\phi(k) = \tan^{-1}(y_k/x_k)$ denotes the phase. Since the QPSK modulated symbols b_m are assumed to be statistically independent, i.i.d random variables, the linear mapping operation such as IDFT performed on b_m also exhibits the characteristics of gaussian random process. Therefore according to the central limit theorem [22], the resulting real x_k and imaginary y_k components of the complex baseband OFDM signal $s_k, k = 1, 2, \cdots, N_F$ after IDFT preprocessing are gaussian and mutually uncorrelated if N_F is chosen to be sufficiently large [23]. The distribution of the complex gaussian symbols can be characterized as zero mean and variance given by $\sigma_b^2 = \frac{1}{2}\mathbb{E}\{|b_m|^2\}, \forall m$ as the variance is distributed among the complex components. Under these conditions, the magnitudes of the complex OFDM signal $a_k, k = 1, 2, \cdots, N_F$, tends to follow the Rayleigh distribution [23]. Now based on the definition of PAPR, the ratio of the peak instantaneous power to average power of an OFDM symbol can be represented by

$$\frac{a_k^2}{2\sigma_b^2} \tag{2.16}$$

(2.16) is a chi-squared distribution with two degrees of freedom. Each degree of freedom is associated with individual complex component x_k^2/σ_b^2 and y_k^2/σ_b^2 . Chi-squared distributions are useful in computing cumulative distribution function (CDF)which determines the probability of occurrence of an event bounded by certain upper threshold limit. The statistical approach allows to determine the probability that the OFDM signal power exceeds PA's dynamic range of operation using complementary cumulative distribution function (CCDF). The probability that the chi-squared distribution χ of a time domain OFDM signal consisting of N_F samples is below certain threshold χ_0 is equivalent to the probability that each of N_F sample is below the given threshold. The chi-squared function χ_k for the k^{th} subcarrier is given by

$$\chi_k = (x_k^2/\sigma_b^2) + (y_k^2/\sigma_b^2).$$

Considering $\chi_{max} = \max(\chi_1, \chi 2, \cdots, \chi N_F)$ to be the chi-squared value of the sample with highest magnitude, the CDF of χmax is given by

$$\begin{aligned} f_{\chi_{max}}(\chi) &= Pr(\chi_{max} \leq \chi_0) \\ &= Pr(\chi_1 \leq \chi_0) \cdot Pr(\chi_2 \leq \chi_0) \cdots Pr(\chi_{N_F} \leq \chi_0) \\ &= (1 - e^{-\chi_0})^{N_F}. \end{aligned} \tag{2.17}$$

The statistical analysis of PAPR using CDF can be illustrated by following relation

$$\delta = \frac{\max\limits_{k\in[1,N_F]} |s_k|^2}{\mathbb{E}\{|s_k|^2\}} = \frac{\max\limits_{k\in[1,N_F]} a_k^2}{\mathbb{E}\{2\sigma_b^2\}} \tag{2.18}$$

As the main interest lies in determining the probability that PAPR value exceeds the given threshold value (χ_0), the CCDF for χ_{max} is given by

$$\begin{aligned} \tilde{f}_{\chi_{max}}(\chi) &= Pr(\chi_{max} \geq \chi_0) \\ &= 1 - (1 - e^{-\chi_0})^{N_F}. \end{aligned} \tag{2.19}$$

As (2.19) is valid under the assumption that samples are mutually uncorrelated and number of subcarriers are sufficiently large, the expression does not hold for the bandlimited or oversampled signals because the sampled discrete points may not contain the highest peak that were present in the continuous time domain signal. In case of oversampling the number of samples per OFDM symbols are increased and the oversampling factor α must be taken into account in CCDF calculation. The CCDF of oversampled OFDM symbol can be determined as

$$\tilde{f}_{\chi_{max}}(\chi) = 1 - (1 - e^{-\chi_0})^{\alpha N_F}.$$

PAPR Reduction Techniques

Several PAPR reduction techniques have been studied in the past to address the non-linearities in OFDM systems. The reduction technique to be employed should be selected based on the desired system performance as every reduction technique has its own merits and demerits. Some of the factors to be considered are the PAPR minimizing capability, power enhancement leading to in band and out of band distortion, bit error rate (BER) degradation, loss in data rate, computational complexity etc. Several PA linearizing techniques are developed to balance the trade-off between linearity and power efficiency.

Non-linearities with power amplifiers in OFDM system has been studied in [24] considering OFDM signal modelled as gaussian distribution. Brief introduction of some of the common PAPR reduction techniques classified into two categories *signal distortion technique* and *signal scrambling technique* is presented in the following paragraph.

Signal distortion technique In signal distortion techniques the high peaks in the input signal are directly removed or *chopped-off* before feeding to PA.

- Clipping

Clipping refers to limiting the maximum input signal power to certain predefined threshold [25]. This is the simplest way of controlling PAPR by hard-limiting but introduces nonlinear and out of band distortion degrading the BER performance. Clipping introduces amplitude distortion as source of noise causing both in band and out of band distortion. Out of band radiation is mainly responsible for degrading spectral efficiency. However filtering can be implemented to reduce the out of band distortion but may result in peak regrowth. Number of iterations may be required to achieve desired peak level.

- Peak Windowing

In peak windowing the large peak beyond certain threshold are alleviated by multiplying the large peak portion of signal with the some window function. The commonly used window function are Kaiser, Hamming window. Unlike clipping, the out of band distortion is reduced by limiting the spectral growth into adjacent channel. However, too long windows can increase BER as it affects larger part of signal.

- Peak Cancellation

In the peak cancellation method [26], a reference signal bandlimited to the bandwidth of the transmitted signal is constructed. The high peaks in the signal are reduced by subtracting the time-shifted and scaled version of the reference signal from it. Sinc pulse can be used as a suitable reference signal. This technique does not cause any out of band distortion. But since sinc function is not a time limited, it cannot be used practically. Therefore implementation of peak cancellation requires trade-off between pulse shaping and out of band distortion.

- Random phase updating

Random phase updating algorithm was introduced in [27] for PAPR reduction in OFDM system. As the name suggests, each subcarrier is assigned some randomly generated phase in iterative manner. The PAPR of the OFDM signal is verified with the predefined threshold after each iteration of the phase update. The stoppage criteria of the algorithm is set by the minimum threshold value or the maximum number of iterations.

- Companding

Companding proposed in [28] refers to compression of the signal with large dynamic range at the input in order to process it efficiently through system with limited dynamic range such that the signal's original dynamic range can be reproduced at the output. The OFDM symbols are companded and quantized after the IDFT operation. The quantization depends on the dynamic range of the signal amplitude. Companding technique enhances the quantization resolution of small signals at the cost of reduced resolution of large signals due to the rare occurrence of high peaks.

Signal scrambling technique Signal scrambling technique reduces the PAPR in multicarrier systems by modifying or scrambling the data in various ways and also by altering the phase factor.

- Coding techniques

Coding can be used to scramble the data in a signal. Coding technique uses additional bit sequence (codes) to modify the information signal which reduces the PAPR in OFDM transmitted signal. The extra bits to be transmitted also reduces the data rate of the system. The choice of suitable code sequence requires exhaustive search depending on the number of subcarriers, modulation scheme used, code rate and also the desired minimum PAPR threshold. Other factors to be considered are implementation complexity and error detection/correction capability of the code. Some well known coding schemes used to reduce PAPR are Golay complementary sequence [29], Shapiro-Rudin sequences, Barker codes and Reed-Muller codes [30].

- Selected mapping (SLM)

Selected mapping proposed in [31] generates a set of time domain OFDM signals each modified by unique phase adjustment while all of them represents the same information data to be transmitted. SLM chooses the most suitable signal among the set of signals that corresponds to the minimum PAPR. The receiver requires the knowledge about the choice of transmitted signal, hence a certain identifier is attached along with the information signal. Therefore the objective of selected mapping (SLM) is not to cancel the peaks but reduce the probability of occurrence of high peaks. The demerits of SLM are loss of data rate due to overhead in transmitted data and increased computation complexity for performing IDFT operation on each OFDM signal in the set.

- Partial transmit sequence (PTS)

In partial transmit sequence (PTS) technique proposed in [32], the data bitstream at the input of the IDFT is divided into number of orthogonal sub-blocks. Each blocks are zero padded to compute separate full-length IDFT for each of them and then rotated

by multiplying with a unique and uncorrelated rotation factors. The result is finally combined to obtain low PAPR signal. The task of generating suitable rotation factors depending on the subcarriers in PTS makes it computationally more expensive than the SLM. The overhead is included in transmitted signal to identify the rotation factor of individual sub-block.

2.3. SIMO-OFDM

The system model in this thesis is based on MU single input multiple output (SIMO) architecture with perfect knowledge of instantaneous channel at the transmitter and receiver. The UL transmission in SIMO model considers multiple copies of independently fading transmitted signals from different single antenna users arriving at spatially separated multiple receive antennas at the BS. Independent fading characteristics of multipath ensure low correlation between shifted replicas of transmitted signal at the receiver and is crucial factor for coherent detection. The copies of transmitted signal is received at each receive antenna creating a communication link between each pair of antenna elements. The main objective is to maximize the SNR by extracting the desired user's signal in the presence of noise and the interfering signals. Array gain can be achieved by employing receive beamforming using linear minimum mean square error (LMMSE) filter at the receiver to coherently combine the signals received at different antennas to increase the SNR [33]. The factors contributing to improved data rate in SIMO-OFDM system are - firstly the increased average SNR due to the receive beamforming across N_R antennas and secondly due to the individual contribution of each N_F subcarrier. In MU system with U users, the sum capacity in the presence of interference is given by

$$c = \sum_{u=1}^{U} \sum_{k=1}^{N_F} log_2(1 + \frac{|\mathbf{h}_{u,k}\omega_{u,k}|^2 P_{u,k}}{\sum_{y\neq u}^{U} |\mathbf{h}_{y,k}\omega_{u,k}|^2 P_{y,k} + \sigma_n^2 |\omega_{u,k}|^2}), \tag{2.20}$$

where $\mathbf{h}_{u,k}$ and $\omega_{u,k}$ are the flat-fading channel coefficient and receive beamformer vector respectively across N_R antennas for the k^{th} subcarrier of user u, $P_{u,k}$ is the power allocated to the k^{th} subcarrier of user u and σ_n^2 is the noise variance.

The total interference to a particular user is the summation of thermal noise and all the other signals in the same frequency band (co-channel interference) arriving from interfering users at a given instant. The total received power of any user should overcome the margin set by the total interference in order to extract the information successfully. The LMMSE equalizer at the receiver scales each received symbol by certain weight such that the scaling should amplify the desired user's signal and attenuate every individual interference, thereby increasing the SINR. The TX-RX joint optimization with full CSI eliminates the interference and performs per subcarrier power loading to the guarantee target BER.

2.4. Adaptive Power Allocation in OFDMA

Power Control in the 4G UL transmission is an irrefutable part of a radio resource management that affects the system performance in both BS and MT. The role of

power control at user end is to increase the power efficiency of MT and to increase the overall system capacity along with interference management at the BS. In case of channel dependent scheduling, if the user has a poor SINR channel, then instead of assigning more power to maintain high data rate and QoS, the approach is to simply reduce the data rate and allocate just sufficient power to sustain the link. The users with the better channel are able to attain high data rate and so the system favors them to make the most out of this opportunity. Therefore the strategy dictates that the power should not be too high causing high co-channel interference to other users and also not too low such that the signal is buried in noise beyond recovery. Unsuccessful transmission demands retransmission of data wasting the spectral efficiency.

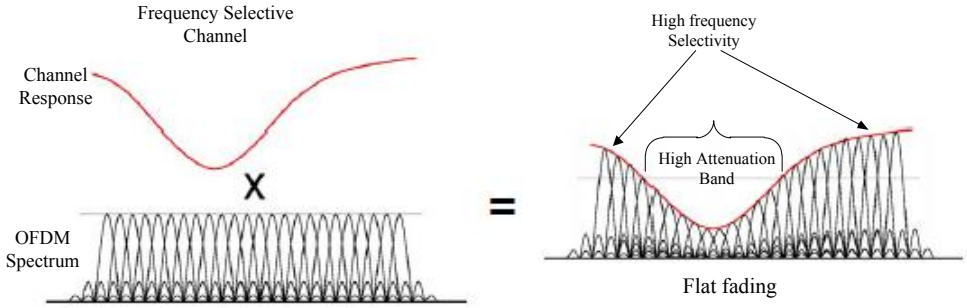

Figure 2.6: Frequency selective fading.

Fig. 2.6 shows the breaking down of single wideband channel frequency response into multiple narrowband flat fading response due to presence of multiple carriers (subcarriers). The high frequency selectivity band has high channel gains providing high SINR links. This is the appropriate band for high data transmission. The high attenuation band has low channel gain. Transmission using this band requires high power to maintain the acceptable SINR. Furthermore, it requires high amplification at the receiver which enhances the noise highly in this band increasing the overall noise overall noise variance. The system performance can be increased by avoiding this band for transmission. The strategy here is to improve the overall system capacity in best possible way and keep the transmit power low. According to 3GPP specifications, the power control in LTE is essential for interference mitigation. Each subcarrier in OFDMA system undergoes independent fading depending on the channel frequency response causing some subcarriers to have high channel gain while some suffer from deep fade. The overall performance of the OFDMA system is determined as an aggregated contribution of each subcarrier.

Adaptive OFDMA is the technique of modifying the characteristics such as modulation, code rate, transmission power of individual subcarrier to improve the energy efficiency and spectral efficiency of the OFDMA system depending on the subcarrier's fading state. The available total power can be distributed among the subcarriers as per their requirement to maintain reliable transmission. The spectral efficiency of a particular subcarrier with high channel gain can be increased accordingly by using high order modulation and high code rate without increasing the transmission power while spectral efficiency of the subcarrier with poor channel gain can be reduced to maintain the link reliability [34]. Therefore an overall improvement in system performance in terms of high spectral efficiency or high data rate can be achieved when there are more

high SINR links.

The SIMO-OFDM system considered in this thesis uses the concept of adaptive OFDMA for optimal power allocation for varying the power and data rate of each subcarrier with respect to its corresponding channel gain. In context of power allocation the word *subcarrier* is used to refer to the frequency domain data symbols i.e. before performing IDFT and the channel gains are the flat-fading channel frequency responses that scales the frequency domain symbols. In this thesis, the sum power and PAPR minimization problem is solved for MU SIMO-OFDMA system with full CSI such that minimum data rate is guaranteed for each user. The channel fading coefficient of all users are assumed to be mutually independent and power allocation is based on the TX-RX optimization such that the subcarrier with strong fading coefficient is allocated sufficiently enough power and those in deep fade is deprived of high power allocation. In MU scenario the power allocated to certain subcarrier of a user is an interference to the corresponding subcarriers (same frequency band) of every other users as shown in 2.20. Hence the optimal power allocation should be sufficient to maintain the QoS for each user while at the same time it should not be high enough causing adverse effect for other users. The SINR in MU SIMO-OFDMA system is an interference coupled function of power and channel gain, and can be decoupled down to the subcarrier level. Therefore instantaneous SINR is used as the performance metric to quantify each link quality and also to dynamically adjust the appropriate power for each subcarrier at that instant. The problem formulation for achieving minimum sum power in a interference coupled system with fixed and variable SINR constraint is discussed in Chapter 4.

Increasing the UL power of a user can certainly increase the QoS for that particular user but at the cost of increased co-channel interference for all other users transmitting on same frequency band. Furthermore, the interference may be experienced by not only for other users at the serving BS (intra-cell co-channel interference) but also by the users at the neighboring BS (inter-cell co-channel interference). Intra-cell co-channel interference can be avoided in OFDMA by performing orthogonal user allocation such that no two users in the same cell transmit using same set of subcarriers. For minimizing the interference, the transmit power can be minimized just enough to maintain the reliable transmission such that the user specific requirement is met.

The MT adjusts power allocated to each subcarrier based on the feedback received from the BS in centralized fashion. Centralized processing at the BS requires the channel information of all the users and can be preferable as the BS is considered to have sufficiently enough power compared to battery operated MT. Such feedback based power allocation is called *closed loop power control* where BS calculates the appropriate power and then instructs each user terminal through DL channel to transmit at given power. The feedback from receiver however have few disadvantages such as the feedback information to be transmitted introduces overhead and also feedback information may be outdated by the time transmitter utilizes it. However the centralized approach can be utilized by minimizing the size of the overhead and regulating the duration between consecutive feedbacks based on the rate at which channel changes. The appropriate power adjustment using adaptive OFDMA plays vital role in utilizing the available transmission power in the best possible way and minimize the PAPR factor for improving power efficiency of signal processing operations.

2.5. Power Minimization Problem

Joint Power Allocation and Beamforming Problem with fixed SINR constraint

This section introduces the joint optimization of transmit power control and receiver beamforming vectors with fixed SINR constraint. The power associated with each user is highly responsible for increasing the interference among other users transmitting in corresponding subcarrier. The iterative algorithm designed as constrained convex optimization problem minimizes the total sum power of all the users by distributing (increasing or decreasing) the power among the subcarriers based on per subcarrier requirement to achieve minimum target rate. If the data rate achieved by particular subcarrier is higher than the target rate, then it can reduce its power and this extra power is distributed among the needy subcarriers. The algorithm iterates until the minimum possible sum power is achieved. Both the parameters (transmit power and receive beamformers) need to be adjusted in coordination with each other as the achievable minimum power may vary for each set of receive beamforming vectors. Hence the degradation in the system performance due to MU interference is dealt by adjusting the power and receive beamformers alternately. Firstly, starting from initial feasible power allocation, the algorithm computes the optimal receive beamformers and then minimizes the power for the fixed obtained beamformers. In the second stage, the minimized power at previous stage is fixed and is used to calculate the new receive beamformers vectors. The process is iterated until convergence such that the optimal (minimal) power allocation and target SINR is achieved. Such alternating approach to jointly optimize power allocation and receive beamformers has been discussed in [35].

The receive beamformer for the k^{th} subcarrier of the u^{th} user is computed as

$$\boldsymbol{\omega}_{u,k} = (\sum_{u=1}^{U} \boldsymbol{\lambda}_{u,k} P_{u,k} \boldsymbol{\lambda}_{u,k}^{H} + \sigma_n^2)^{-1} \boldsymbol{\lambda}_{u,k} \tag{2.21}$$

at each iteration for fixed given power. Then the power allocation optimization problem to determine optimal power allocation $P_{u,k}$, where $u = 1, 2, \cdots, U$ and $k = 1, 2, \cdots, N_F$ for fixed beamforming vectors is given by

$$\begin{aligned} \underset{P}{\text{minimize}} \quad & \sum_{u=1}^{U} \sum_{k=1}^{N_F} P_{u,k} \\ \text{subject to} \quad & \\ & P_{u,k} |\boldsymbol{\omega}_{u,k}^{H} \boldsymbol{\lambda}_{u,k}|^2 \geq \\ & \gamma_{min} (\sum_{y \neq u}^{U} P_{y,k} |\boldsymbol{\omega}_{u,k}^{H} \boldsymbol{\lambda}_{y,k}|^2 + \sigma_n^2 \|\boldsymbol{\omega}_{u,k}\|^2) \quad \forall u, k. \end{aligned} \tag{2.22}$$

The constraint is defined by SINR formulation for the k^{th} subcarrier of the u^{th} user given by

$$\text{SINR}_{u,k} \geq \gamma_{min} \quad \forall u, k,$$

where γ_{min} is the minimum SINR threshold for each subcarrier and $\text{SINR}_{u,k} = \frac{P_{u,k}|\boldsymbol{\omega}_{u,k}^H \boldsymbol{\lambda}_{u,k}|^2}{\sum_{y\neq u}^{U} P_{y,k}|\boldsymbol{\omega}_{u,k}^H \boldsymbol{\lambda}_{y,k}|^2 + \sigma_n^2 \|\boldsymbol{\omega}_{u,k}\|^2}$. For fixed beamforming vector problem, the constraint in (2.22) is reduced to

$$
\begin{aligned}
P_{u,k}|\boldsymbol{\lambda}_{u,k}|^2 &\geq \gamma_{min}\Big(\sum_{y\neq u}^{U} P_{y,k}|\boldsymbol{\lambda}_{y,k}|^2 + \sigma_n^2\Big) \\
P_{u,k}|\boldsymbol{\lambda}_{u,k}|^2 - \gamma_{min}\sum_{y\neq u}^{U} P_{y,k}|\boldsymbol{\lambda}_{y,k}|^2 &\geq \gamma_{min}\sigma_n^2 \\
P_{u,k} - \gamma_{min}\frac{\sum_{y\neq u}^{U} P_{y,k}|\boldsymbol{\lambda}_{y,k}|^2}{|\boldsymbol{\lambda}_{u,k}|^2} &\geq \gamma_{min}\frac{\sigma_n^2}{|\boldsymbol{\lambda}_{u,k}|^2}.
\end{aligned}
$$

The above equation can be expressed in compact form for k^{th} subcarrier as

$$
[\mathbf{I}_{(U)} - \boldsymbol{\Psi}^k]\mathbf{p}^k \geq \mathbf{a}^k \quad \forall k, \tag{2.23}
$$

where $\boldsymbol{p}^k \in \mathbb{C}^U$ is a column vector containing positive powers at the k^{th} subcarrier i.e. $P_{u,k}, u = 1, 2, \cdots, U$, $\boldsymbol{a}^k$ is the positive column vector with elements $a_u^k = \gamma_{min}\frac{\sigma_n^2}{|\boldsymbol{\lambda}_{u,k}|^2} \in \mathbb{C}^U, u = 1, 2, \cdots, U$ at the k^{th} subcarrier. $\boldsymbol{\Psi}^k$ is the normalized channel gain matrix for the k^{th} subcarrier given by

$$
\boldsymbol{\Psi}_{uy}^k = \begin{cases} 0 & \text{if} \quad u = y \\ \gamma_{min}\frac{|\lambda_{y,k}|^2}{|\lambda_{u,k}|^2} & \text{if} \quad u \neq y \end{cases}
$$

The problem (2.22) minimizes the sum power of all the users across all subcarriers while maintaining SINR above γ_{min} which is equivalent to finding the minimal power vector $\mathbf{p}^k \; \forall k$ such that (2.23) is satisfied. Similar centralized power allocation algorithms are discussed in [36, 37]. According to Perron-Frobenius theory of nonnegative matrix, if matrix $\boldsymbol{\Psi}^k \; \forall k$ is irreducible, then there exists a positive power vector $\hat{\mathbf{p}}^k \; \forall k$ such that $[\mathbf{I}_{(U)} - \boldsymbol{\Psi}^k] \; \forall k$ is invertible and positive and given SINR target vector is feasible [38]. Hence the inequality constraint achieving optimal power vector is given by

$$
\hat{\mathbf{p}}^k = [\mathbf{I}_{(U)} - \boldsymbol{\Psi}^k]^{-1}\mathbf{a}^k \quad \forall k. \tag{2.24}
$$

The Perron-Frobenius theorem states that the minimum eigenvalue that satisfies (2.24) corresponds to the maximum value of $\boldsymbol{\gamma}_{min}$ i.e. the spectral radius of $\boldsymbol{\Psi}^k \; \forall k$ should be less than 1 or equivalently $\rho(\boldsymbol{\Psi}^k) < 1 \; \forall k$ in order to have feasible power vector $\hat{\mathbf{p}}^k$ [38].

The power minimization steps are shown in **Algorithm** 1. The algorithm initialization requires feasible power allocation $P_{u,k}^{(0)}$ such that the user specified QoS is satisfied. Receive beamforming vectors of minimum mean square error (MMSE) weights

are calculated using the current power allocation matrix. The new optimal power allocation matrix $P^*_{u,k}\ \forall u,k$ is calculated by solving optimization problem (2.22) for fixed receive beamforming vectors. Then the power allocation matrix of current iteration is used as a starting point for next iteration and same steps are repeated until convergence. The algorithm is guaranteed to converge to yield minimum power allocation matrix.

Algorithm 1 Joint Power and Beamforming Problem with fixed SINR constraint

1: Set γ_{min} (QoS)
2: Initialize $\hat{P}_{u,k} = P^{(0)}_{u,k} \quad u = 1, 2, \cdots, U, \quad k = 1, 2, \cdots, N_F$
3: **repeat**
4: Calculate
MMSE weight $\boldsymbol{\omega}_{u,k}\ \forall u,k$ using (3.16)
5: Solve optimization problem (2.22) for $P^*_{u,k} \quad \forall u,k$
6: Update $\hat{P}_{u,k} = P^*_{u,k}\ \forall u,k$
7: **until** Convergence

2.6. Multiple Access with OFDMA

Multiple Access schemes in wireless system governs the way multiusers share the available radio resources in the bandwidth limited system. It defines the system's optimal strategy for serving multiple users in a network such that every active user is given fair share of priority and the available resources are shared efficiently among the users. Resources can be identified as the channels allocated for two terminals to communicate with each other and multiple access strategies further decides on the quality of service to be provided on this particular channel. Orthogonal frequency division multiple access OFDMA is a multiuser system where the resources are shared in basis of OFDM principles. The communication channels between two terminals, mainly BS and MT can be classified into two groups in terms of duplexing. Firstly, the UL channel also known as multiple access channel (MAC), where the channel is used to transfer data from multiple MTs to single serving BS and secondly DL channel also known as broadcast channel (BC), where the channel is used to transfer data from single serving BS to multiple MTs. The scope of this thesis is limited to UL OFDMA system. Each multiple user in an UL system can be distinguished by their respective channel and generally the resource allocation strategy of multiple access scheme depends on the quality of this channel.

In contrast to OFDM, OFDMA further decomposes each OFDM symbol down to subcarrier level, thus increasing the shareable resource components among the users at a given time. For illustration OFDM symbol can be visualized as number of blocks in a 2 dimensional (2D) time-frequency grid where each block represents individual data bearing orthogonal subcarrier in an OFDM symbol as shown in Fig. 2.7.

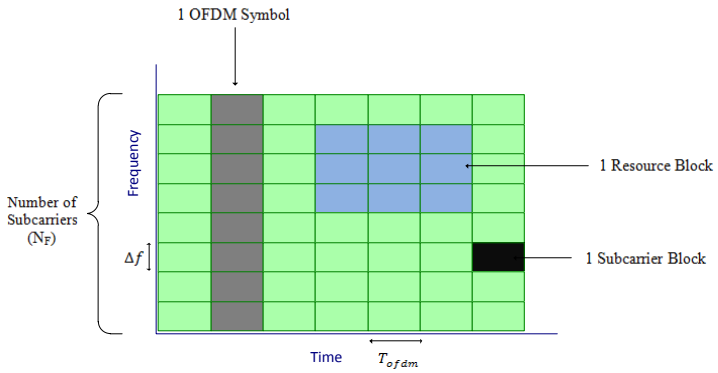

Figure 2.7: OFDMA Time-Frequency grid.

The number of blocks in the frequency axis is equivalent to the number of subcarriers and frequency separation between adjacent subcarriers is Δf. In the time axis each block belongs to different OFDM symbols with the separation of T_{ofdm}. Further during the transmission each of these blocks are separated in spatial domain identified by unique flat-fading channel gain (spatial signature). The multiple users in OFDMA system are able to communicate simultaneously where each user is assigned a group of subcarrier blocks. This group of subcarrier blocks is called *resource block* according to LTE terminology. The frequent CSI feedback at the transmission ends allows to perform dynamic resource allocation on the basis of channel quality. The OFDMA subcarriers can be modified to accommodate wide range of bandwidths, by controlling the DFT size N_F and subcarrier spacing Δf. Therefore a reliable multiple access technique enhances the system performance by using only those subcarriers that can maximize the utilization of the available limited resources and also implement a optimal way of assigning each of these resource blocks to the demanding users.

Due to increasing popularity of OFDM modulation scheme in recent communication technologies, OFDMA has become a subject of extensive research. The OFDMA was introduced as a potential multiple access technique for future generation mobile communication with the practical implementation in community antenna television (CATV) networks by [39] in 1998. Since then OFDMA has been implemented in numerous wireless standards such as IEEE 802.20 [40], European Telecommunications Standards Institute (ETSI) broadband radio access networks [41], digital video broadcasting (DVB) for UL transmission [42], satellite communications [43] and also used for DL communication in 4G cellular system such as WiMAX [44] and LTE [7].

2.7. OFDMA and SC-FDMA

The 3GPP Evolved Universal Terrestrial Radio Access (E-UTRA) has specified the performance targets for 4G systems as per the LTE specification. Based on 4G specification, OFDM is the multicarrier modulation technique proposed for the PHY implementation. Therefore two eligible candidates chosen for multiple access schemes are (OFDMA) for the DL and SC-FDMA for the UL. The difference between these two schemes and their respective characteristics that inspired altered choice is discussed in this section.

The parameters used for comparison between OFDMA and SC-FDMA are capacity, outage probability but the most important parameter among all is peak-to-average

power ratio (PAPR). The MTs transmitting on UL channel are more vulnerable to PAPR because high PAPR tends to drain an excessive amount of battery life as discussed in Section 2.2.3.2. PAPR does not impose much of a threat on BS but it is crucial to maintain low PAPR on MTs during UL transmission. Therefore PAPR is considered the main reason for 3GPP to suggest SC-FDMA as an alternative to OFDMA for UL transmission.

SC-FDMA is an OFDMA based system where transmitted symbol poses a single carrier behavior obtained by DFT spreading. SC-FDMA is based on the single carrier frequency domain equalization (SC-FDE) modulation scheme, which is a variant of OFDM and differs in a way that the IDFT block from the transmitter is moved to receiver. The noteworthy feature here is that the complex baseband symbols are mapped to 2^{N_Q}-ary constellation in time domain. The receiver takes IDFT of received symbols to perform frequency domain equalization and again converts it back to time domain using DFT. Therefore both of these schemes perform channel equalization in frequency domain. The main reason for occurrence of high PAPR in OFDM system is due to the superimposition of complex exponentials during IDFT operation causing random fluctuation of peak power with respect to the average power. The removal of IDFT block in case of SC-FDE simply prevents occurrence of high PAPR. SC-FDMA is able to achieve low PAPR on average due to mapping of the complex baseband signal in time domain i.e. transmitting the symbols in their original domain [44].

Resource Allocation in SC-FDMA compared to OFDMA

The flexible resource allocation in OFDMA system with N_F subcarriers is associated with the parallel existence of each orthogonal subcarrier in different frequency bands within a given OFDMA symbol period T_{ofdm}. In other words each low rate baseband symbol is positioned parallelly across the entire channel (transmission) bandwidth. This is the concept of flat fading that provides robustness against the multipath fading and it relates to the time-invariant nature of the subcarriers during the duration T_{ofdm}. Fig. 2.8 shows the difference between OFDMA and SC-FDMA in terms of symbol distribution in time-frequency plane. In case of SC-FDMA, the temporally mapped symbols are transmitted in series at the rate of N_F times the OFDMA, hence occupies larger bandwidth as per the concept of single carrier. However, SC-FDMA utilizes the advantage of parallel transmission as in OFDMA and transmits same amount of symbols in given symbol duration. In SC-FDMA system, the transmitter and receiver both contains pair of DFT and IDFT processing blocks. An extra DFT processing is performed to spread the time domain complex baseband symbols across N_F subcarriers. Each serial time domain SC-FDMA symbol transmits N_F parallel sub-symbols positioned parallelly across entire channel bandwidth with the frequency spacing of Δf. Therefore, even though SC-FDMA transmits each symbol at high rate, the N_F subcarriers remain constant during the overall SC-FDMA symbol duration T_{scfdma} in a similar way, the parallel subcarriers coexist during the overall OFDMA symbol duration T_{ofdma} in case of OFDMA. This constant nature of subcarrier in SC-FDMA, inherits the multicarrier transmission property of OFDMA. The remaining processing stages are as same as that in OFDMA resulting in the time domain symbols. At the receiver, detection is performed using DFT and IDFT block in reverse order compared to transmitter. Due to the parallel decomposition of the physical resources, the resource allocation can be done in similar ways as discussed in Section 2.4.

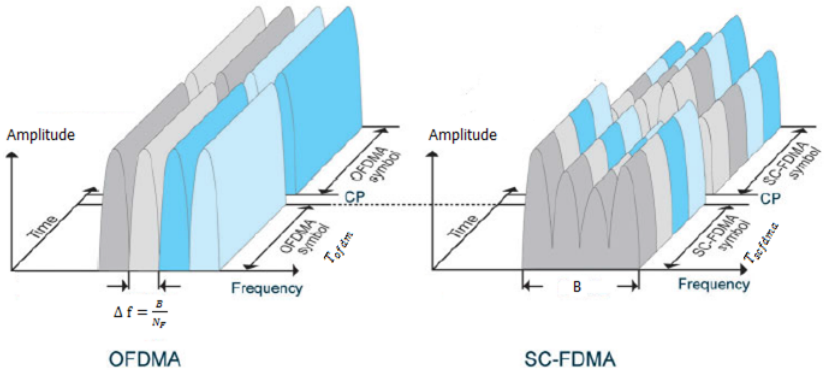

Figure 2.8: OFDMA vs SC-FDMA [21].

OFDMA acknowledges the original domain of the complex baseband symbol as frequency domain and conversion to time domain before transmission results in high PAPR in time domain. It is shown in [45] that in case of localized subcarrier allocation, the PAPR of SC-FDMA decreases by 2-3 dB compared to general OFDMA. Thus SC-FDMA possess the characteristics of OFDMA while maintaining low PAPR. Nonetheless OFDMA too has significant advantages over SC-FDMA. Robustness against frequency-selective fading allows OFDMA to achieve higher data rate per subcarrier yielding better sum-rate capacity. SC-FDMA is more vulnerable to frequency-selective fading due to large transmission bandwidth. Further in the case of SC-FDMA, the DFT spreading induces high PAPR in frequency domain due to phase offset mismatch caused by frequency offset and random phase noise. This leads to large fluctuation in *out of band power* leading to inter-subcarrier interference, adjacent channel interference and narrowband co-channel interference [46].

3. SYSTEM MODEL AND SIMULATION SETUP

This chapter describes the simulation setup with the help of system model and the mathematical representation of UL single cell OFDMA system. The thesis considers the Continuous Rate UL Power Allocation problem. The main objective is to develop a power allocation algorithm for MU OFDM system that minimizes the sum power consumption of all users over all allocated subcarriers. The algorithm presented in the thesis investigates PAPR aware power minimization given the minimum rate constraint per user. It states that the sum power is minimized such that the desired user specific QoS is achieved. The thesis proposes the centralized nature such that the power allocation is performed at the central entity i.e. the BS. The general block diagram of SIMO UL OFDMA system with the mathematical description is presented in the following sections.

3.1. System Model

The system model shown in Fig. 3.1 depicts a single cell MU UL SIMO-OFDMA system consisting of U single antenna users and a base station with N_R antennas. The OFDMA system consists of N_F subcarriers allocated to each user. We assume the CSI is known at the receiver. The overall system is divided and described in two parts namely transmitter and receiver.

3.1.1. Transmitter

In this section, the transmitter side of the the system model is considered. The original data stream of length N_D to be transmitted by each user u is denoted by $\mathbf{x}_u, u = 1, 2, \cdots, U$. Each user's symbol vector $\mathbf{x}_u$ is mapped onto the signal constellation depending on 2^{N_Q}-ary scheme. The mapped serial data stream is converted into N_F complex baseband parallel bitstreams denoted by $b_{u,k}, k = 1, 2, ...N_F$ hence resulting in complex vector corresponding to user u across N_F subcarriers as

$$\mathbf{b}_u = [b_{u,1}, b_{u,2}, \cdots, b_{u,N_F}]^{\mathrm{T}} \in \mathbb{C}^{N_F}. \tag{3.1}$$

The subcarrier mapping stage corresponds to power allocation in SIMO precoding where a certain power based on the power allocation matrix of individual user is allocated to each subcarrier.

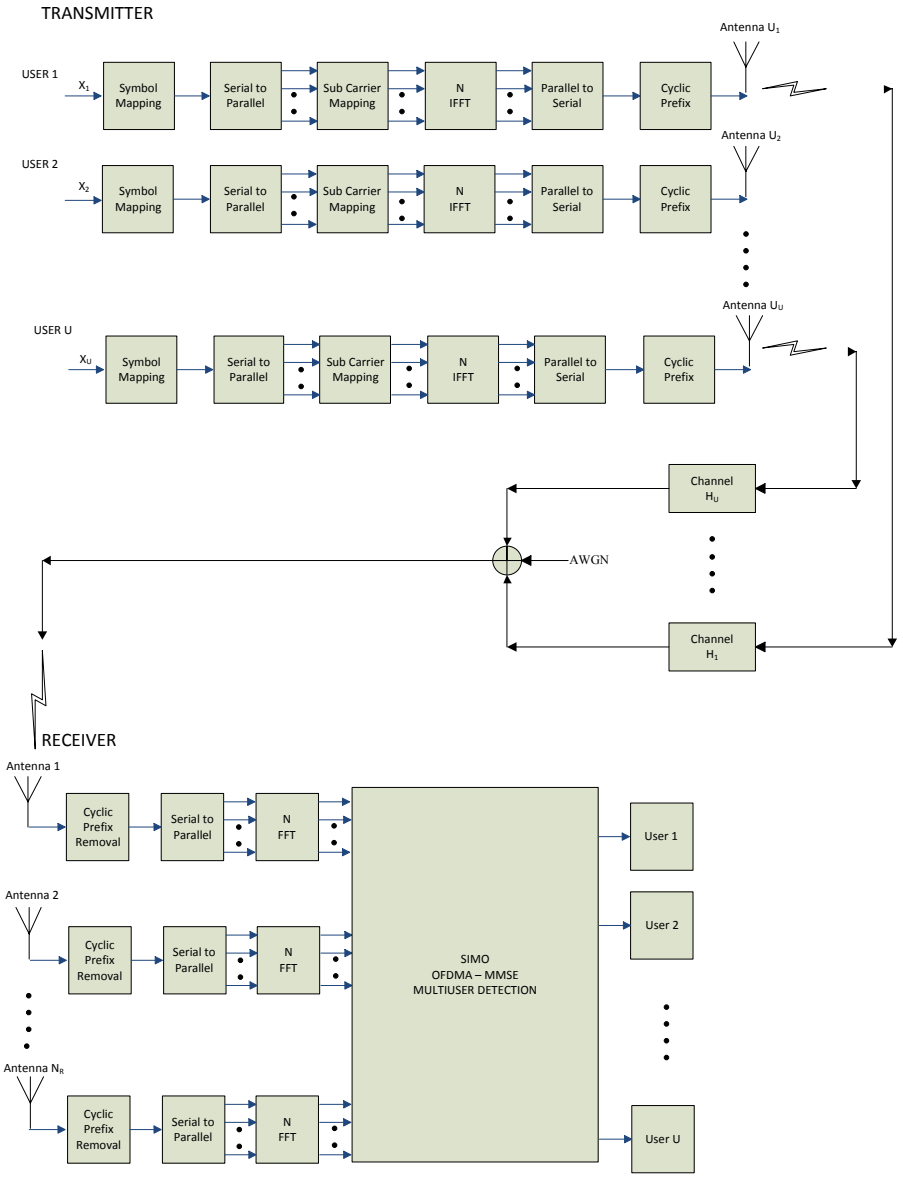

Figure 3.1: System Model for multiuser Uplink OFDMA.

The power allocation matrix of user u is given by

$$\mathbf{P}_u = \begin{pmatrix} P_{u,1} & 0 & \dots & 0 \\ 0 & P_{u,2} & \dots & 0 \\ \vdots & \vdots & \ddots & \vdots \\ 0 & 0 & \dots & P_{u,N_F} \end{pmatrix}_{N_F \times N_F}$$

The power allocation is performed by multiplying frequency domain parallel bitstream of user u by $\sqrt{\mathbf{P}_u}$ where $\mathbf{P}_u$ is the power allocation matrix for user u. Each diagonal element $P_{u,k}$ of the matrix $\mathbf{P}_u$ is power allocated to the k^{th} subcarrier of user u. The overall power matrix P is arranged as

$$\mathbf{P} = \begin{bmatrix} \boxed{\begin{matrix}\text{Power Allocation}\\ \text{Matrix for User 1}\\ \mathbf{P}_1\end{matrix}} & & & \\ & \boxed{\begin{matrix}\text{Power Allocation}\\ \text{Matrix for User 2}\\ \mathbf{P}_2\end{matrix}} & & \\ & & \ddots & \\ & & & \boxed{\begin{matrix}\text{Power Allocation}\\ \text{Matrix for User u}\\ \mathbf{P}_U\end{matrix}} \end{bmatrix}_{UN_f \times UN_F}$$

The IDFT block modulates each bitstream on individual subcarrier with orthogonal frequencies and combines them resulting in the time domain signal that constitutes the actual OFDM symbol. It is accomplished by multiplying the bit loaded bitstream with the IDFT matrix $\mathbf{F}^{-1}$. The DFT matrix $\mathbf{F} \in \mathbb{C}^{N_F \times N_F}$ is represented by complex exponentials over the range of frequencies where each element of the matrix is given by

$$f_{k,m} = \frac{1}{\sqrt{N_F}} e^{(i2\pi(m-1)(k-1)/N_F)}, \tag{3.2}$$

where $k, m = 1, 2, \cdots, N_F$ and $\frac{1}{\sqrt{N_F}}$ is the normalization factor. The complex OFDM modulated discrete time samples for user u at the k^{th} subcarrier can be expressed as

$$s_{u,k} = \frac{1}{\sqrt{N_F}} \sum_{m=1}^{N_F} b_{u,m} \sqrt{P_{u,m}} e^{(i2\pi(m-1)(k-1)/N_F)}. \tag{3.3}$$

The matrix visualization of the transmitted OFDM symbol can be shown as

$$\underbrace{\begin{matrix}\text{OFDM}\\ \text{Symbols}\end{matrix}\begin{bmatrix} s_{u,1} \\ s_{u,2} \\ \vdots \\ s_{u,k} \end{bmatrix}}_{N_F \times 1} = \underbrace{\begin{matrix}\text{IDFT}\\ \end{matrix}\begin{bmatrix} f_{1,1} & f_{2,1} & \cdots & f_{N_F,1} \\ f_{1,2} & f_{2,2} & \cdots & f_{N_F,2} \\ \vdots & \vdots & \ddots & \vdots \\ f_{1,N_F} & f_{2,N_F} & \cdots & f_{N_F,N_F} \end{bmatrix}}_{N_F \times N_F} \underbrace{\begin{matrix}\text{Parallel}\\ \text{User Data}\end{matrix}\begin{bmatrix} x_{u,1} \\ x_{u,2} \\ \vdots \\ x_{u,m} \end{bmatrix}}_{N_F \times 1} \underbrace{\begin{matrix}\text{T}\\ \text{Power Allocation}\end{matrix}\begin{bmatrix} \sqrt{P_{u,1}} & 0 & \cdots & 0 \\ 0 & \sqrt{P_{u,2}} & \cdots & 0 \\ \vdots & \vdots & \ddots & \vdots \\ 0 & 0 & \cdots & \sqrt{P_{u,N_F}} \end{bmatrix}}_{N_F \times N_F}$$

where $f_{k,m}$ is defined in (3.2). In a more compact form it can be written as

$$\mathbf{s}_u = \mathbf{F}^{-1}\sqrt{\mathbf{P}_u}\mathbf{b}_u \in \mathbb{C}^{N_F}. \tag{3.4}$$

Final stage of the transmitter is addition of CP to alleviate the ISI. Assuming the number of channel taps (multipaths) be L, then the minimum CP length required by the OFDM system to imitate the circular convolution property of DFT after transmission through time domain channel is $N_{CP} \geq (L-1)$. In this simulation, instead of inserting CP physically in the transmitted sequence, the affect of CP is realized by multiplying the transmitted bit of each user with their respective circulant channel matrix $\mathbf{H}_u$ constructed from channel taps of length L. The topic is discussed in detail in Section 3.1.2.

3.1.2. Receiver

The reception of OFDM symbol starts with the removal of CP. The symbols are assumed to be received without the loss of orthogonality amongst subcarrier and without offset in carrier frequency. The received time domain OFDM symbol after the CP removal can be expressed as

$$\mathbf{r} = \sum_{u}^{U} \mathbf{H}_u \mathbf{F}^{-1}\sqrt{\mathbf{P}_u}\mathbf{b}_u + n, \tag{3.5}$$

where $\mathbf{r} \in C^{N_R N_F \times 1}$ is the received symbol vector for all users across N_R antennas, $\mathbf{F}^{-1}\mathbf{P}_u^{1/2}\mathbf{b}_u \in C^{N_R N_F \times 1}$ is the transmitted symbol vector for the u^{th} user across N_R antennas, $\mathbf{H}_u \in C^{N_R N_F \times N_F}$ is the space time channel matrix of time domain channel impulse response (CIR) for the u^{th} user across N_R antennas and $\mathbf{n} \sim \mathcal{CN}(0, \sigma_n^2 I_{N_R N_F}) \in C^{N_R N_F \times 1}$ is the identically distributed and uncorrelated additive white gaussian noise with variance σ_n^2. Equation (3.5) can be decomposed to express desired user content as

$$\mathbf{r}_u = \mathbf{H}_u \mathbf{F}^{-1}\sqrt{\mathbf{P}_u}\mathbf{b}_u + \sum_{y \neq u}^{U} \mathbf{H}_y \mathbf{F}^{-1}\sqrt{\mathbf{P}_y}\mathbf{b}_y + \mathbf{n}. \tag{3.6}$$

The first term in (3.6) is the desired part of the received signal to be extracted. The second term is the co-channel interference caused by the other users transmitting at the corresponding subcarrier.

The SIMO UL MAC consists of individual circulant channel matrix $\mathbf{H}_u^r$ for the u^{th} user across each receive antenna r and it can be written as $\mathbf{H}_u = [\mathbf{H}_u^1, \mathbf{H}_u^2, \ldots, \mathbf{H}_u^{N_R}]^{\mathrm{T}} \in \mathbb{C}^{N_R N_F \times N_F}$ where $\mathbf{H}_u^r = circ[h_{u,1}^r, h_{u,2}^r, \ldots, h_{u,L}^r, 0_{1\times N_F - L}]^{\mathrm{T}} \in \mathbb{C}^{N_F \times N_F}$. L denotes the length of channel taps i.e. number of multipath fading coefficients. The interaction between the u^{th} user's transmitted symbol vector $\mathbf{s}_u$ and L-tap channel $\mathbf{H}_u^r$ for receive antenna r can be visualized using matrix as

$$\underbrace{\begin{bmatrix} r^r_{u,1} \\ r^r_{u,2} \\ \vdots \\ r^r_{u,k} \end{bmatrix}}_{N_F \times 1} = \underbrace{\begin{bmatrix} h^r_{u,1} & h^r_{u,N_F} & \dots & h^r_{u,L} & \dots & h^r_{u,2} \\ h^r_{u,2} & h^r_{u,1} & \ddots & \ddots & \ddots & \vdots \\ \vdots & \ddots & \ddots & \ddots & & h^r_{u,L} \\ h^r_{u,L} & & \ddots & \ddots & \ddots & \vdots \\ \vdots & \ddots & & \ddots & \ddots & h^r_{u,N_F} \\ h^r_{u,N_F} & \dots & h^r_{u,L} & \dots & h^r_{u,2} & h^r_{u,1} \end{bmatrix}}_{H^r_u \in \mathbb{C}^{N_F \times N_F}} \underbrace{\begin{bmatrix} s_{u,1} \\ s_{u,2} \\ \vdots \\ s_{u,k} \end{bmatrix}}_{N_F \times 1} + n_{(N_F \times 1)}$$

where $s_{u,k}$ is the time domain sample transmitted at k^{th} subcarrier of user u and $r^r_{u,k}$ is a copy of the sample of transmitted OFDM symbol of user u received at the k^{th} subcarrier of receive antenna r. Element $h^r_{u,k}$ denotes the complex time domain fading coefficients or CIR such that $h^r_{u,k} = 0 for L < k \leq N_F$. The received vector results from circular convolution between transmitted symbol and CIR.

The next step is to transform the received symbols back to frequency domain to retain the original user data stream for SIMO detection using minimum mean square error equalizer in frequency domain (MMSE-FDE). This is accomplished by the DFT block in the OFDM system. The received symbol vector $\mathbf{r}$ is converted to frequency domain by multiplying with the DFT matrix $\mathbf{F}_{N_R} = \mathbf{I}_{N_R} \otimes \mathbf{F} \in \mathbb{C}^{N_R N_F \times N_R N_F}$, where $\otimes$ is the kronecker product. $\mathbf{F}_{N_R}$ is a block diagonal matrix consisting of N_R blocks of the DFT matrix $\mathbf{F}$ suitable for multiplying each N_R block of received vector $\mathbf{r}$ separately.

$$\tilde{\mathbf{r}} = \mathbf{F}_{N_R} \mathbf{r}. \tag{3.7}$$

MMSE-FDE requires the $N_F \times N_F$ time domain CIR to be transformed into frequency domain CFR. This allows decoupling of channels such that the output across N_F subcarriers are parallel flat fading SIMO channels achieving spatial multiplexing by using properties of MIMO spatial channel.

According to the convolution theorem, *multiplication with circulant matrix in time domain* is equivalent to the *multiplication with the diagonal matrix in frequency domain*. Exploiting the above property along with the property of DFT, it is known that eigenvectors of a circulant matrix of a given size are the columns of DFT matrix of same size. This property can be used in decoupling of time domain circulant channel into parallel frequency domain channel coefficient. The eigenvalue decomposition is performed on time domain circulant channel $\mathbf{H}_u$ as

$$\mathbf{\Gamma}_u = \mathbf{F}_{N_R} \mathbf{H}_u \mathbf{F}^{-1}, \tag{3.8}$$

where $\mathbf{\Gamma}_u = [\mathbf{\Gamma}^1_u, \mathbf{\Gamma}^2_u, \dots, \mathbf{\Gamma}^{N_R}_u]^{\mathrm{T}} \in \mathbb{C}^{N_R N_F \times N_F}$ and $\mathbf{\Gamma}^r_u = diag[\lambda^r_{u,1}, \lambda^r_{u,2}, \dots, \lambda^r_{u,N_F}] \in \mathbb{C}^{N_F \times N_F}$. Each element of diagonal matrix $\mathbf{\Gamma}^r_u$ are the complex channel frequency response coefficient. This aids in analyzing received sample in each subcarrier as a corresponding transmitted sample scaled by the scalar complex fading coefficient given by the eigenvalues. Each fading coefficient can be expressed as

$$\lambda_{u,k}^{r} = \frac{1}{\sqrt{N_F}} \sum_{l=1}^{L} h_{u,l}^{r} e^{i2\pi(l-1)(k-1)/N_F}, k = 1, \ldots, N_F, \tag{3.9}$$

where $\lambda_{u,k}^{r}$ is the eigenvalue or the channel frequency response of the k^{th} subcarrier of the u^{th} user at receive antenna r and $h_{u,l}^{r} \in \mathbb{C}^{L}$ are the non-zero elements in $h_{u,k}^{r} \in \mathbb{C}^{N_F}$. Further consider vector $\boldsymbol{\lambda}_{u,k} \in \mathbb{C}^{N_R}$ where $\boldsymbol{\lambda}_{u,k} = [\lambda_{u,k}^{1}, \lambda_{u,k}^{2}, \ldots, \lambda_{u,k}^{N_R}]^{\mathrm{T}}$. The eigenvalue is determined for each element of SIMO channel taps and used to construct an entire frequency domain channel matrix $\boldsymbol{\Gamma} = [\boldsymbol{\Gamma}_1, \boldsymbol{\Gamma}_2, \ldots, \boldsymbol{\Gamma}_U] \in \mathbb{C}^{N_R N_F \times U N_F}$ as

$$\boldsymbol{\Gamma} = \begin{array}{c} \\ N_R 1 \\ N_R 2 \\ \\ N_R r \end{array} \begin{array}{c} \begin{array}{cccc} User1 & User2 & & Useru \end{array} \\ \left[\begin{array}{c|c|c|c} \boldsymbol{\Gamma}_1^1 & \boldsymbol{\Gamma}_2^1 & \cdots & \boldsymbol{\Gamma}_u^1 \\ \hline \boldsymbol{\Gamma}_1^2 & \boldsymbol{\Gamma}_2^2 & \cdots & \boldsymbol{\Gamma}_u^2 \\ \hline \vdots & \vdots & \vdots & \vdots \\ \hline \boldsymbol{\Gamma}_1^r & \boldsymbol{\Gamma}_2^r & \cdots & \boldsymbol{\Gamma}_U^{N_R} \end{array}\right]_{N_R N_F \times U N_F} \end{array}$$

The frequency domain received signal for the u^{th} user can be derived as

$$\begin{aligned} \tilde{\mathbf{r}}_u &= \mathbf{F}\mathbf{r}_u \\ &= \mathbf{F}_{N_R}(\mathbf{H}_u \mathbf{F}^{-1} \sqrt{\mathbf{P}_u}\mathbf{b}_u + \sum_{y \neq u}^{U} \mathbf{H}_y \mathbf{F}^{-1} \sqrt{\mathbf{P}_y}\mathbf{b}_y + \mathbf{n}) \\ &= \underbrace{\mathbf{F}_{N_R}\mathbf{H}_u\mathbf{F}^{-1}} \sqrt{\mathbf{P}_u}\mathbf{b}_u + \sum_{y \neq u}^{U} \mathbf{F}_{N_R}\mathbf{H}_y\mathbf{F}^{-1} \sqrt{\mathbf{P}_y}\mathbf{b}_y + \mathbf{F}_{N_R}\mathbf{n} \\ &= \boldsymbol{\Gamma}_u \sqrt{\mathbf{P}_u}\mathbf{b}_u + \sum_{y \neq u}^{U} \boldsymbol{\Gamma}_y \sqrt{\mathbf{P}_y}\mathbf{b}_y + \tilde{\mathbf{n}}. \end{aligned} \tag{3.10}$$

Focusing on user u, the frequency domain received signal at the k^{th} subcarrier of receive antenna r can be expressed as

$$\tilde{r}_{u,k}^{r} = \lambda_{u,k}^{r} \sqrt{P_{u,k}} b_{u,k} + \sum_{y \neq u}^{U} \lambda_{y,k}^{r} \sqrt{P_{y,k}} b_{y,k} + \tilde{n}_k^r. \tag{3.11}$$

3.2. MMSE-FDE Detection

The MMSE filter estimates the transmitted symbol based on minimizing the mean square error (MSE) by Bayesian approach using the *a priori* information from re-

ceived data assuming that both received vector $\tilde{\mathbf{r}}$ and transmitted vector $\mathbf{b}$ are random variables with known joint statistics. The Bayesian approach utilizes the *a priori* probability distribution function (pdf) of $\mathbf{b}$ and conditional pdf of $(\mathbf{r}|\mathbf{b})$ to determine the *a posteriori* pdf of $\mathbf{b}$ given by $(\mathbf{b}|\mathbf{r})$. The MMSE calculates the estimate $\hat{\mathbf{b}}$ as a conditional expectation $\mathbb{E}\{(\mathbf{b}|\mathbf{r})\}$ of $\mathbf{b}$ given $\mathbf{r}$ based on the *a posteriori* probability.

The simulations consider the multiuser SIMO linear MMSE-FDE scheme for the equalization of the received symbol vector. Orthogonality among the subcarriers is an important factor for the optimum performance of the equalizer. The Linear SIMO detection is performed across each subcarrier defined by parallel flat fading narrowband channels by quantizing each received symbol to the nearest constellation points as hard outputs. OFDM system uses one-tap FDE to equalize the symbols that undergo frequency-selective fading channel. The MMSE equalizer is able to suppress the noise enhancement in low SNR regime approaching matched filter receiver while in high SNR regime it approaches zero forcing (ZF). The MU-SIMO detection is same as single user detection except the multiuser interference should be taken under consideration.

The equalizer calculates estimators $\mathbf{\Omega}_u = [\mathbf{\Omega}_u^1, \mathbf{\Omega}_u^2, \ldots, \mathbf{\Omega}_u^{N_R}]^{\mathrm{T}} \in \mathbb{C}^{N_R N_F \times N_F}$ where $\mathbf{\Omega}_u^r = diag[\omega_{u,1}^r, \omega_{u,2}^r, \ldots, \omega_{u,N_F}^r] \in \mathbb{C}^{N_F \times N_F}$ where $\omega_{u,k}^r$ is the MMSE estimator for the transmitted symbol at the k^{th} subcarrier of the u^{th} user arriving at the r^{th} receive antenna. The filtered signal of the u^{th} user at the k^{th} subcarrier given the linear estimator $\boldsymbol{\omega}_{u,k} \in \mathbb{C}^{N_R}$ can be expressed as

$$\hat{b}_{u,k} = \boldsymbol{\omega}_{u,k}^H \tilde{r}_{u,k}, \tag{3.12}$$

where $\boldsymbol{\omega}_{u,k} = [\omega_{u,k}^1, \omega_{u,k}^2, \ldots, \omega_{u,k}^{N_R}]^{\mathrm{T}}$. The minimization of the MSE error can be formulated as

$$\begin{aligned} minimize \quad & \mathrm{Tr}\,\mathbb{E}\{(\hat{b}_{u,k} - b_{u,k})(\hat{b}_{u,k} - b_{u,k})^H\} = \\ minimize \quad & \mathrm{Tr}\,\mathbb{E}\{(\omega_{u,k}^H \tilde{r}_{u,k} - b_{u,k})(\omega_{u,k}^H \tilde{r}_{u,k} - b_{u,k})^H\} \end{aligned} \tag{3.13}$$

The MMSE estimator $\mathbf{\Omega}_u$ is found by minimizing (3.13) with respect to the variable $\mathbf{\Omega}$ and is given by

$$\mathbf{\Omega}_u = (\mathbf{A}_{\tilde{R}\tilde{R}})^{-1} \mathbf{A}_{\tilde{R}b_u} \tilde{\mathbf{r}}_u, \tag{3.14}$$

where $\mathbf{A}\{\cdot\}$ denotes autocorrelation matrix, $\mathbf{A}_{\tilde{r}\tilde{r}} \in \mathbb{C}^{N_R N_F \times N_R N_F}$ is the autocorrelation matrix of received signal of all receiving antennas and $\mathbf{A}_{\tilde{r}b_u} \in \mathbb{C}^{N_R N_F \times N_F}$ is the cross-correlation matrix between received symbol and transmitted symbol of the u^{th} user.

$$\mathbf{A}_{\tilde{r}\tilde{r}} = \mathbf{\Gamma}_u \mathbf{P}_u \mathbf{\Gamma}_u^H + \sum_{y \neq u}^{U} \mathbf{\Gamma}_y \mathbf{P}_y^{1/2} \mathbf{\Gamma}_y^H + \sigma_n^2 \mathbf{I}_{(N_F N_R)}$$
$$= \boxed{\mathbf{\Gamma} \mathbf{P} \mathbf{\Gamma}^H + \sigma_n^2 \mathbf{I}_{(N_F N_R)}}. \tag{3.15}$$

$$\mathbf{A}_{\tilde{r}b_u} = \boxed{\mathbf{\Gamma}_u \sqrt{\mathbf{P}_u}}.$$

Using (3.12), (3.14) and (3.15), the MMSE estimate of the u^{th} user at the k^{th} subcarrier for each receive antenna r can be written as

$$\hat{b}_{u,k} = \underbrace{[(\sum_{u=1}^{U} \lambda_{u,k} P_{u,k} \lambda_{u,k}^H + \mathbf{I}_{N_R} \sigma_n^2)^{-1} \lambda_{u,k} \sqrt{P_{u,k}}]^H}_{\omega_{u,k}^H} \tilde{r_{u,k}}, \tag{3.16}$$

which can be written in more compact form in per user context as

$$\hat{\mathbf{b}}_u = \boxed{[(\mathbf{\Gamma} \mathbf{P} \mathbf{\Gamma}^H + \sigma_n^2 \mathbf{I}_{(N_F N_R)})^{-1} \mathbf{\Gamma}_u \sqrt{\mathbf{P}_u}]^H \tilde{\mathbf{r}}}. \tag{3.17}$$

3.3. SINR

In a SIMO system, the average SNR increase is proportional to the number of receive antennas. The per user signal to interference plus noise ratio (SINR)for the k^{th} subcarrier is calculated by aggregating channel gain $\boldsymbol{\lambda}_{u,k} \in \mathbb{C}^{N_R}$ and filter coefficients $\boldsymbol{\omega}_{u,k} \in \mathbb{C}^{N_R}$ at the k^{th} subcarrier of each receive antenna r.

$$\gamma_{u,k} = \frac{\mathbb{E}\{\tilde{r}_{u,k} \tilde{r}_{u,k}^H\}}{\mathbb{E}[I_{u,k} I_{u,k}^H]}$$

$$= \frac{\mathbb{E}\{(\boldsymbol{\omega}_{u,k}^H \boldsymbol{\lambda}_{u,k} \sqrt{P_{u,k}} b_{u,k})(\boldsymbol{\omega}_{u,k}^H \boldsymbol{\lambda}_{u,k} \sqrt{P_{u,k}} b_{u,k})^H\}}{\mathbb{E}\{(\sum_{y \neq u}^{U} \boldsymbol{\omega}_{u,k}^H \boldsymbol{\lambda}_{y,k} \sqrt{P_{y,k}} b_{y,k} + \boldsymbol{\omega}_{u,k}^H \tilde{n}_{u,k})(\sum_{y \neq u}^{U} \boldsymbol{\omega}_{u,k}^H \boldsymbol{\lambda}_{y,k} \sqrt{P_{y,k}} b_{y,k} + \boldsymbol{\omega}_{u,k}^H \tilde{n}_{u,k})^H\}}$$

$$= \frac{\boldsymbol{\omega}_{u,k}^H \boldsymbol{\lambda}_{u,k} \sqrt{P_{u,k}} \mathbb{E}\{b_{u,k} b_{u,k}^H\} (\sqrt{P_{u,k}})^H \boldsymbol{\lambda}_{u,k}^H \boldsymbol{\omega}_{u,k}}{\sum_{y \neq u}^{U} \boldsymbol{\omega}_{u,k}^H \boldsymbol{\lambda}_{y,k} \sqrt{P_{y,k}} \mathbb{E}\{b_{y,k} b_{y,k}^H\} (\sqrt{P_{y,k}})^H \boldsymbol{\lambda}_{y,k}^H \boldsymbol{\omega}_{u,k} + \boldsymbol{\omega}_{u,k} \mathbb{E}\{\tilde{n}_{u,k} \tilde{n}_{u,k}^H\} \boldsymbol{\omega}_{u,k}^H}$$

$$= \frac{\boldsymbol{\omega}_{u,k}^H \boldsymbol{\lambda}_{u,k} P_{u,k} \boldsymbol{\lambda}_{u,k}^H \boldsymbol{\omega}_{u,k}}{\sum_{y \neq u}^{U} \boldsymbol{\omega}_{u,k}^H \boldsymbol{\lambda}_{y,k} P_{y,k} \boldsymbol{\lambda}_{y,k}^H \boldsymbol{\omega}_{u,k} + \boldsymbol{\omega}_{u,k}^H \sigma_n^2 \boldsymbol{\omega}_{u,k}}$$

$$= \frac{P_{u,k}|\boldsymbol{\omega}_{u,k}^H \boldsymbol{\lambda}_{u,k}|^2}{\sum_{y\neq u}^{U} P_{y,k}|\boldsymbol{\omega}_{u,k}^H \boldsymbol{\lambda}_{y,k}|^2 + \sigma_n^2 \|\boldsymbol{\omega}_{u,k}\|^2}. \tag{3.18}$$

3.4. Capacity

MIMO is an attractive technique of increasing capacity in high SNR regime proportional to N_{min} spatial degrees of freedom, where N_{min} is the minimum number of transmitter and receiver antennas [47]. SIMO model considered in the simulation may not contribute significantly to capacity gain due to single antenna at the transmitter. The sum rate capacity of MU-SIMO in *bits/sec/Hz* can be expressed as

$$\begin{aligned} \mathbf{c}_u &= \sum_{k=1}^{N_F} \log_2(1 + \frac{P_{u,k}|\boldsymbol{\omega}_{u,k}^H \boldsymbol{\lambda}_{u,k}|^2}{\sum_{y\neq u}^{U} P_{y,k}|\boldsymbol{\omega}_{u,k}^H \boldsymbol{\lambda}_{y,k}|^2 + \sigma_n^2 \|\boldsymbol{\omega}_{u,k}\|^2}) \\ &= \sum_{k=1}^{N_F} \log_2(1 + \gamma_{u,k}), \end{aligned} \tag{3.19}$$

where $\gamma_{u,k}$ is the SINR of the u^{th} user at the k^{th} subcarrier.

3.5. PAPR

The power distribution of the transmitted OFDM symbol is analyzed by performing spectral decomposition over different orthogonal subcarriers and acknowledging the contribution of each subcarrier to the average power of signal. The PAPR as discussed in detail in Section 2.2.3.2. It can be formulated as the ratio of the peak power and the average power of the complex OFDM modulated signal $\mathbf{s}_u$. It is expressed as

$$\begin{aligned} \delta_u &= \frac{\max(|s_u|^2)}{1/N_F \sum_{k=1}^{N_F} \mathbb{E}\{|s_u|^2\}} \\ &= \frac{\max(|s_u|^2)}{1/N_F \sum_{k=1}^{N_F} P_{u,k}}, \end{aligned} \tag{3.20}$$

where $\max(|s_u|^2)$ is the peak power for user u and $P_{u,k}$ is the k^{th} diagonal element from the power allocation matrix of user u.

4. PROBLEM FORMULATION AND OPTIMIZATION

In this chapter, the optimization problems are formulated on the basis of the system model described on Chapter 3. The iterative algorithms are designed to continuously adjust the power at each subcarrier of each user $P_{u,k}$ based on various constraints with main concern to minimize power along with the PAPR. The algorithms compute power for all users in a centralized manner at the receiver provided CSI of all the users in the system.

4.1. Joint Power Allocation and Beamforming Problem with SINR and Rate constraint

The power minimization problem with fixed SINR constraint was discussed in . However, fulfilling the high throughput requirement in presence of harsh propagation channel requires more robust algorithms because fixed SINR algorithms may not be able to provide feasible solution in these scenarios. This section introduces a modification of optimization problem (2.22) with additional per user minimum rate constraint (R_u) as a QoS metric and SINR as a variable. The data rate $c_{u,k}$ for the k^{th} subcarrier of the u^{th} user can be expressed as a function of the SINR $\gamma_{u,k}$ as

$$c_{u,k} = \log_2(1+\gamma_{u,k}).$$
$$\mathbf{c}_u = \sum_{k=1}^{N_F} \log_2(1+\gamma_{u,k}).$$

The per user data rate $\mathbf{c}_u$ is decomposed into subcarrier level where each subcarrier is defined by parallel flat fading channel coefficient. Therefore unlike the fixed SINR target in Section 2.5, here the SINR target varies for different subcarriers of different users. The power is transferred among the subcarriers of each user u depending on their channel coefficient such that the aggregated rate for every user is maintained above the given threshold R_u. The new modified optimization problem can be expressed as

$$\begin{aligned} \underset{P,\,\gamma}{\text{minimize}} \quad & \sum_{u=1}^{U}\sum_{k=1}^{N_F} P_{u,k} \\ \text{subject to} \quad & \\ & \sum_{k=1}^{N_F} \log_2(1+\gamma_{u,k}) \geq R_u \quad \forall u \\ & \frac{P_{u,k}|\boldsymbol{\omega}_{u,k}^H \boldsymbol{\lambda}_{u,k}|^2}{\sum_{y\neq u}^{U} P_{y,k}|\boldsymbol{\omega}_{u,k}^H \boldsymbol{\lambda}_{y,k}|^2 + \sigma_n^2 \|\boldsymbol{\omega}_{u,k}\|^2} \geq \gamma_{u,k} \quad \forall u,k \end{aligned} \tag{4.1}$$

4.1.1. Convexity

In this section the concept of convexity is introduced to solve the power control problem (4.1). Convex optimization refers to minimization of convex function over a set of

convex constraints.

Convex Functions: A function $f(x)$: $\mathbb{R}^n \rightarrow \mathbb{R}$ is said to be convex if for any two points $x, y \in \mathbb{R}^n$

$$f(\theta x + (1-\theta)y) \leq \theta f(x) + (1-\theta)f(y), \quad \forall \theta \in [0,1]. \tag{4.2}$$

The function f is convex if the line segment joining the points $(x, f(x))$ and $(y, f(y))$ is always above the graph of function f. The function f is said to be concave if $-f$ is convex.

Convex Sets: A set $S \subset \mathbb{R}^n$ is said to be convex if for any two points $x, y \in S$ also lies in S and can be expressed as

$$\theta x + (1-\theta)y \in S, \quad \forall \theta \in [0,1] \quad \text{and} \quad x, y \in S. \tag{4.3}$$

First order Taylor series: If function f is continuously differentiable, then the convexity of function f is defined by first order Taylor series given by

$$f(y) \geq f(x) + \nabla f(x)^T (y - x), \quad \forall x, y \in S, \tag{4.4}$$

where $f(x) + \nabla f(x)^T (y - x)$ is an affine function of y that represents the first order Taylor approximation of y in neighbourhood x. The linear approximation is a global underestimator of convex function. The optimization variable $x \in \mathbb{R}^n$ is said to be feasible in given domain S if $x \in S$ and it satisfies all equality and inequality constraints. The optimal solution x^* is considered to be a global minimum if $f(x^*) \leq f(x)$ [48].

4.1.2. Log-Convex Transformation

The SINR constraint in power minimization problem (4.1) is an interference coupled function as described in [49]. According to [50] the impact of interference coupling in wireless system results in competition among the users to maximize their own utility with no regard to other users. Further it is confirmed that the competitive nature of users results in *loss of convexity* or the interference coupled SINR function are neither convex nor concave in power domain. Hence the problem (4.1) cannot be solved using convex optimization techniques in its given form however it can be transformed into a convex optimization problem such that the achieved optimal solution reflects the desired solution to the original problem. In this thesis the convex property of the interference coupled SINR function is exploited by transforming the problem (4.1) into log-domain based on COV. Log-convexity can be used to solve non-convex problems using convex optimization techniques and it has been previously investigated in [51, 52].

Here the transformation to logarithmic power domain refers to COV required for the implementation of log-convexity.

$$P_{u,k} = e^{\alpha_{u,k}} \quad \forall u, k$$

Due to the monotonicity of the logarithm function, every positive element of power vector $P_{u,k}$ is associated with a unique $\alpha_{u,k}$. The objective in problem (4.1) now becomes summation of exponential terms $e^{\alpha_{u,k}}\ \forall u,k$, which is convex. After the transformation and taking natural logarithm on both sides of the SINR constraint, the new SINR constraint can be expressed as

$$\alpha_{u,k} + 2\ln|\omega_{u,k}^H \lambda_{u,k}| - \ln(\sum_{y\neq u}^{U} |\omega_{u,k}^H \lambda_{y,k}|^2 e^{\alpha_{y,k}} + \sigma_n^2 |\omega_{u,k}\|^2) \geq \ln\gamma_{u,k} \quad \forall u,k. \quad (4.5)$$

The third term in left hand side (LHS) of (4.5) is a convex and can be represented in the form of log-sum-exponential form as

$$\ln(\sum_{y\neq u}^{U} e^{ln(|\omega_{u,k}^H \lambda_{y,k}|^2 e^{\alpha_{y,k}})} + e^{\ln(\sigma_n^2 \|\omega_{u,k}\|^2)})$$
$$\Leftrightarrow \ln(\sum_{y\neq u}^{U} e^{(\alpha_{y,k} + 2\ln|\omega_{u,k}^H \lambda_{y,k}|)} + e^{ln(\sigma_n^2 \|\omega_{u,k}\|^2)})$$

Altogether LHS of (4.5) is concave. Moreover the RHS of (4.5) is also concave. Therefore it results in non-convex constraint and requires SCA to approximate it as a convex. The problem can be solved by linear approximation of the concave part $\ln\gamma_{u,k}$ in RHS at a feasible point $\hat{\gamma}_{u,k}$. Since linear approximation always overestimates the concave function, the solution results in the best convex upper bound. Let the concave part in RHS be denoted by $f(\gamma_{u,k})$. The linear approximation of $f(\gamma_{u,k})$ at a point $\hat{\gamma}_{u,k}$ is given by

$$f(\gamma_{u,k}, \hat{\gamma}_{u,k}) = \ln\hat{\gamma}_{u,k} + \frac{(\gamma_{u,k} - \hat{\gamma}_{u,k})}{\hat{\gamma}_{u,k}} \quad \forall u,k \quad (4.6)$$

The new transformed convex optimization problem for variable SINR can be expressed as

$$\begin{aligned}
&\underset{\alpha,\,\gamma}{\text{minimize}} \quad \sum_{u=1}^{U}\sum_{k=1}^{N_F} e^{\alpha_{u,k}} \\
&\text{subject to} \\
&\qquad \sum_{k=1}^{N_F} \log_2(1+\gamma_{u,k}) \geq R_u \quad \forall u \qquad (4.7) \\
&\qquad \alpha_{u,k} + 2\ln|\omega_{u,k}^H \lambda_{u,k}| - \ln(\sum_{y\neq u}^{U} |\omega_{u,k}^H \lambda_{y,k}|^2 e^{\alpha_{y,k}} + \\
&\qquad \sigma_n^2 \|\omega_{u,k}\|^2) \geq f(\gamma_{u,k}, \hat{\gamma}_{u,k}) \quad \forall u,k
\end{aligned}$$

The algorithm for joint optimization of TX-RX follows the steps as shown in **Algorithm** 2. The algorithm requires a feasible initialization i.e. feasible power allocation

$P_{u,k}^{(0)}\ \forall u,k$ such that R_u is satisfied. RX and SINR is calculated for given power allocation. Then the optimization solves the SCA problem at some feasible point $\gamma_{u,k}^{*}\ \forall u,k$ in the vicinity of $\hat{\gamma}_{u,k}$ for fixed RX. The achieved minimum power $\hat{P}_{u,k}\ \forall u,k$ is used as a new initial feasible power allocation and the whole process is repeated until convergence. Thus the accuracy of the approximation is improved by iterating the optimization problem until convergence. The algorithm is guaranteed to converge to some local optimum. Similar approach and its proof of convergence is shown in [53].

Algorithm 2 Joint Power and Beamforming Problem with SINR and Rate constraint

1: Set R_u (user-specified QoS)
2: Initialize $\hat{P}_{u,k} = P_{u,k}^{(0)} \quad u = 1, 2, \cdots, U, \quad k = 1, 2, \cdots, N_F$
3: **repeat**
4: Calculate
RX $\omega_{u,k}\ \forall u,k$ using (3.16)
SINR $\hat{\gamma}_{u,k}\ \forall u,k$ using (3.18)
5: Solve optimization problem (4.7) for $\alpha_{u,k}^{*}, \gamma_{u,k}^{*} \quad \forall u,k$
6: Update
$\hat{P}_{u,k} = e^{\alpha_{u,k}^{*}} \quad \forall u,k$
7: **until** Convergence

4.2. PAPR aware Joint Power Allocation and Beamforming Problem with SINR and Rate constraint

This section introduces a PAPR aware optimization problem with additional SPV constraint to the problem (4.1). This is an intuitive approach of statistically reducing the dispersion or variability among the discrete time domain samples $s_{u,k}$, where $u = 1, 2, \cdots, U$ and $k = 1, 2, \cdots, N_F$ for respective user u such that the PAPR at the transmitter is reduced. The optimal power allocation is now constrained by a SPV threshold. The PAPR can be controlled at the power allocation stage in frequency domain. The SPV for user u can be expressed as

$$\sigma_{P_u}^2 = \frac{2}{N_F^2} \sum_{\substack{p,q=1 \\ q>p}}^{N_F} P_{u,p} P_{u,q} \quad \forall u, \tag{4.8}$$

The complete derivation of (4.8) is shown in Appendix 1. Using (4.8), the SPV can be minimized by allocating all the power to a single subcarrier. In other words, concentrating all the power on single subcarrier yields the same PAPR as that of single carrier system. Using (A1.1), (A1.2) and (A1.3), the affect of SPV constraint on PAPR of user u can be shown as

$$\lim_{P_{u,n}\to\infty} \frac{\max(|s_u|^2)}{\frac{1}{N_F}\sum_{k=1}^{N_F} P_{u,k}} = 1,$$

where $P_{u,n}$ can be any $n = 1, 2, \cdots, N_F$ bearing highest initial power.

4.2.1. Notion of multi-objective programming (MOP) and Pareto optimality

Multi-objective programming (MOP) refers to optimization problem consisting of multiple objectives to be optimized simultaneously. In case when objectives have conflicting nature, it is difficult or almost impossible to find a global optimizer. Such problems can be solved to yield various solutions that represent the acceptable trade-off and compromise between the objectives. Defining optimality in MOP requires introduction to concept of Pareto optimality. Here since no global optimal solution exists that satisfies all the multiple objectives, a Pareto-optimal solution is determined based on some relaxation technique. A solution is said to be Pareto optimal if there exists no feasible solution for which improvement in one objective does not lead to a simultaneous degradation in one or more of the other objectives. The set consisting of all Pareto optimal points is called Pareto set.

4.2.2. Solving PAPR Aware optimization problem

- Relaxing the SPV constraint

The proposed relaxation technique changes the structure of the objective such that now it is defined by weighted aggregated function of sum power and the SPV to form a MOP problem. The structure of the new objective can be expressed as

$$\theta_1(\sum_{u=1}^{U}\sum_{k=1}^{N_F} P_{u,k}) + \theta_2\sigma_P^2. \tag{4.9}$$

The objective in (4.9) is a convex function formed by the linear combination of sum power and SPV variable where each objective term is weighted by a scalar θ_i to form a meaningful aggregation such that $\theta_i \geq 0, i = 1, 2, \cdots, n$ and $\sum_{i=1}^{n} \theta_i = 1$ where n is the number of terms in the objective. In this case $n = 2$. Now depending on desired minimization preference, weight θ_i on each objective can be adjusted. The global minimizer of the entire MOP objective, ν^* is a Pareto-optimal point which might be very difficult to realize but maximizing the weight (θ_i), an optimal minimizer $\hat{\nu}^*$ can be determined that concentrates only on minimizing the i^{th} term in objective without much influence from the other terms having smaller weights. The new optimization problem for PAPR aware scenario can be expressed as

$$
\begin{aligned}
&\underset{P,\,\gamma,\,\sigma_P^2}{\text{minimize}} \quad \theta(\sum_{u=1}^{U}\sum_{k=1}^{N_F} P_{u,k}) + (1-\theta)\sigma_P^2 \\
&\text{subject to} \\
&\qquad \sum_{k=1}^{N_F} \log_2(1+\gamma_{u,k}) \geq R_u \quad \forall u \\
&\qquad \frac{P_{u,k}|\omega_{u,k}^H \lambda_{u,k}|^2}{\sum_{y\neq u}^{U} P_{y,k}|\omega_{u,k}^H \lambda_{y,k}|^2 + \sigma_n^2 \|\omega_{u,k}\|^2} \geq \gamma_{u,k} \quad \forall u,k \\
&\qquad \frac{2}{N_F^2}\sum_{\substack{p,q=1 \\ q>p}}^{N_F} P_p P_q \leq \sigma_P^2
\end{aligned}
\tag{4.10}
$$

The problem (4.10) is solved by minimizing over different values of $\theta \in [0,1]$ to generate different optimal solutions $\hat{\nu}^*$ in Pareto set which aids in analyzing the trade-off between power allocation and SPV. Log-convex transformation follows the COV of power $P_{u,k} = e^{\alpha_{u,k}} \quad \forall u,k$ and SINR constraint is implemented as discussed in Section 4.1.2. The SPV constraint can be implemented in the form

$$
\frac{2}{N_F^2}\sum_{\substack{p,q=1 \\ q>p}}^{N_F} e^{\alpha_p+\alpha_q} \leq \sigma_P^2 \tag{4.11}
$$

LHS in (4.11) is a summation of exponentials and RHS is a scalar. Hence, SPV constraint is convex. The PAPR aware power minimization problem (4.10) can be solved as a convex problem as

$$
\begin{aligned}
&\underset{\alpha_{u,k},\,\gamma_{u,k},\,\sigma_P^2}{\text{minimize}} \quad \theta(\sum_{u=1}^{U}\sum_{k=1}^{N_F} e^{\alpha_{u,k}}) + (1-\theta)\sigma_P^2 \\
&\text{subject to} \\
&\qquad \sum_{k=1}^{N_F} \log_2(1+\gamma_{u,k}) \geq R_u \quad \forall u \\
&\qquad \alpha_{u,k} + 2\ln|\omega_{u,k}^H \lambda_{u,k}| - \ln(\sum_{y\neq u}^{U} |\omega_{u,k}^H \lambda_{y,k}|^2 e^{\alpha_{y,k}} + \sigma_n^2\|\omega_{u,k}\|^2) \\
&\qquad \geq f(\gamma_{u,k}, \hat{\gamma}_{u,k}) \quad \forall u,k \\
&\qquad \frac{2}{N_F^2}\sum_{\substack{p,q=1 \\ q>p}}^{N_F} e^{\alpha_p+\alpha_q} \leq \sigma_P^2
\end{aligned}
\tag{4.12}
$$

The **Algorithm** 3 shows the complete cycle of operation to achieve the optimal solution for (4.12). The steps in **Algorithm** 3 are same as in **Algorithm** 2. However,

there are few additional parameters. Beside other initializations, the value of $\theta \in [0, 1]$ is also fixed which governs the dependency of optimal solution with respect to the objective terms. The solution of current iteration is used as a feasible starting point for the next iteration. The algorithm is guaranteed to converge to some local optimum.

Algorithm 3 PAPR aware Joint Power and Beamforming Problem with SINR and Rate constraint

1: Set R_u (user-specified QoS)
2: Set $\theta \in [0, 1]$
3: Initialize $\hat{P}_{u,k} = P_{u,k}^{(0)} \quad u = 1, 2, \cdots, U, \quad k = 1, 2, \cdots, N_F$
4: **repeat**
5: Calculate
RX $\omega_{u,k} \ \ \forall u, k$ using (3.16)
SINR $\hat{\gamma}_{u,k} \ \ \forall u, k$ using (3.18)
6: Solve optimization problem (4.12) for $\alpha_{u,k}^*, \gamma_{u,k}^*, \sigma_P^{2^*} \quad \forall u, k$
7: Update
8: Update $\hat{P}_{u,k} = e^{\alpha_{u,k}^*} \ \ \forall u, k$
9: **until** Convergence

5. NUMERICAL ANALYSIS

This chapter discusses the performance of the proposed algorithm based on numerical results obtained from number of simulations. The simulation model for single cell MU SIMO-OFDMA system is set up as per described in Chapter 3. The key parameters and their values used in simulation are shown in table 5.1.

Table 5.1: Simulation Parameters.

Parameter	Symbol	Value
Number of Users	U	3
Number of BS Antenna	N_R	4
Number of User's Antenna		1
Number of Channel Taps	L	3
Noise variance	σ_n^2	1

The goal of the simulations is to find an optimal power allocation for every user in an adaptive OFDMA system such that the power allocation is performed at the subcarrier level. Per user rate constraint is determined as $R_u = N_F R_k$ where R_k is the spectral efficiency or rate per subcarrier. In rest of the section the rate constraint is expressed in terms of R_u since all the simulations are performed at $N_F = 8$. The two main parameters governing the resulting power vector are the QoS being the per user minimum rate constraint R_u and SPV constraint. The **Algorithm** 3 solves a relaxed multi objective convex optimization problem where objective comprises aggregation of sum power and SPV variable. Due to the difficulty in obtaining a global minimizer for the aggregated version of objective, a scaling factor θ_i is used such that $\sum_{i=1}^{n} \theta_i = 1$ where n is the number of terms in the objective. In this case, $n = 2$. The simulation results are shown at different values of parameter θ_i. The feasible initial power allocation should satisfy the QoS constraint before proceeding with the iterative algorithm. For effective PAPR reduction, power of any one of the distinct subcarrier of each user is highly increased. For fair evaluation in terms of PAPR and focusing on the statistical property of the time domain OFDMA symbols, the PAPR is calculated by transmitting the gaussian symbols. To accurately investigate the impacts, the simulation is performed for static channel fading coefficient $h_{u,l}^r$. The time domain channel fading coefficients are included in Appendix 2.

The iterative joint TX-RX optimization is performed to obtain the optimal power allocation. At the beginning of each loop, a new beamforming vector is calculated for the given power vector. Then, the optimal power allocation for each user is determined for fix beamforming vector by solving SCA algorithm. The convergence criteria of the iterative algorithm depends on the difference between the objective function of two successive iterations. The convergence threshold used as a stopping criteria for each loop is set to be 0.0001. The PAPR is calculated for 10^7 random gaussian symbols and its distribution is analyzed using the CCDF $Pr(PAPR > \delta)$ curve.

The user specific QoS based power allocation algorithm as in this simulation depends on the channel gain of individual subcarriers. The higher the channel gain, the better the reception. The simulation assumes perfect estimation of channel state information at the receiver (CSIR) and also perfect synchronization without loss of orthogonality among subcarriers. The LMMSE is used to compute the receive beamformers.

And the overall SINR is determined by combining different copies of transmitted signal arriving at different receive antennas. Therefore the achieved SINR at the particular subcarrier depends on the individual channel gains across all receive antennas. Table 5.2 shows the channel gain $\lambda^r_{u,k}$ of all the subcarriers of all the users across all receive antennas and $\lambda_{u,k} \in \mathbb{C}^{N_R}$ is a channel gain vector for the k^{th} subcarrier of user u.

Table 5.2: Channels Gains.

$\boldsymbol{\lambda}_{u,k}$	$\lvert\lambda^1_{u,k}\rvert^2$	$\lvert\lambda^2_{u,k}\rvert^2$	$\lvert\lambda^3_{u,k}\rvert^2$	$\lvert\lambda^4_{u,k}\rvert^2$
1,1	0.2169	0.3066	0.8196	0.7134
1,2	0.3408	0.1385	0.5132	0.4794
1,3	0.4309	0.0332	0.2087	0.0175
1,4	0.3036	0.1339	0.108	0.4007
1,5	0.1419	0.2646	0.0414	1.031
1,6	0.1713	0.267	0.0243	0.7377
1,7	0.2663	0.257	0.2955	0.0650
1,8	0.2402	0.3218	0.7197	0.2095
2,1	0.0934	0.0444	1.16	0.2597
2,2	0.1243	0.6612	0.8167	0.3108
2,3	0.6586	0.9901	0.329	0.1358
2,4	0.7626	0.4306	0.0592	0.0159
2,5	0.2423	0.1118	0.0506	0.2701
2,6	0.0231	0.6285	0.2312	0.5708
2,7	0.3666	0.8765	0.6101	0.4931
2,8	0.4509	0.3026	1.042	0.2612
3,1	0.2345	0.6052	0.1357	0.0917
3,2	0.0311	0.3314	0.1875	0.0531
3,3	0.4621	0.5619	0.1929	0.2134
3,4	1.622	0.6628	0.1675	0.2596
3,5	2.005	0.2334	0.1283	0.1105
3,6	1.039	0.0241	0.0794	0.0722
3,7	0.1168	0.4993	0.0476	0.2216
3,8	0.1262	0.8814	0.0700	0.2521

Table 5.3 shows the power allocation pattern for equal and unequal initialization methods for $R_u = 2$ and $\theta = 1$. Here only the power is minimized without taking SPV constraint into account. The influence of $\boldsymbol{\lambda}_{u,k}$ can be observed from the data. The final allocated power is such that the sum of power of all users (entire column) is minimized while maintaining the per user minimum rate constraint R_u. The power allocation pattern reflects the orthogonal allocation at low rate constraint. The similarity in the power allocation pattern in both the initialization methods can be observed such that high power is allocated to the channels with high channel gain. For example in case of user 1, the highest power is allocated to subcarrier 1 ($u, k = 1, 1$) having highest channel gain $\boldsymbol{\lambda}_{1,1}$ and the lowest power is allocated to subcarrier 3 ($u, k = 1, 3$) having lowest channel gain $\boldsymbol{\lambda}_{1,3}$.

Table 5.3: Power Allocation at $R_u = 2$, $\theta = 1$.

u, k	Equal Power Initialization		Unequal Power Initialization	
	Initial	Final	Initial	Final
1,1	0.5	0.44233	0.62469	0.46028
1,2	0.5	0.16684	1.7149	0.04728
1,3	0.5	0.00092	0.12499	0.00094
1,4	0.5	0.00093	0.02535	0.00094
1,5	0.5	0.24525	0.80967	0.26333
1,6	0.5	0.09330	0.16761	0.10329
1,7	0.5	0.00093	1.6361	0.00094
1,8	0.5	0.09591	0.54787	0.17883
2,1	0.5	0.00074	0.97488	0.00072
2,2	0.5	0.05309	2.4678	0.1533
2,3	0.5	0.26313	0.55368	0.24844
2,4	0.5	0.00074	0.15969	0.00072
2,5	0.5	0.00070	0.82421	0.00070
2,6	0.5	0.00360	0.58789	0.00359
2,7	0.5	0.3127	0.01543	0.29781
2,8	0.5	0.18412	0.16406	0.10825
3,1	0.5	0.00076	1.2263	0.00076
3,2	0.5	0.00076	1.8931	0.00076
3,3	0.5	0.02564	0.79472	0.02623
3,4	0.5	0.39104	0.99095	0.39097
3,5	0.5	0.35186	0.45632	0.35158
3,6	0.5	0.00075	0.24052	0.00075
3,7	0.5	0.00076	0.45407	0.00076
3,8	0.5	0.00189	0.94342	0.00175

In case of equal power initialization, it can be noticed that, the power allocated to rows $u, k = 1, 2$, $u, k = 1, 5$ and $u, k = 1, 8$ differ from the above discussed point of view. The rows $u, k = 1, 2$ and $u, k = 1, 5$ are more prioritized despite having poor channel gain compared to $u, k = 1, 8$. This phenomenon results due to the presence of high interference in the corresponding subcarrier of other users or simply due to the co-channel interference. The high channel gain in the subcarrier 8 of interfering user $u, k = 2, 8$ imposes high interference to subcarrier 8 of user 1 $u, k = 1, 8$. Since the channel gain for $u, k = 1, 8$ is not sufficient to yield high SINR in the presence of interference, instead of increasing its power, the optimal minimum power can be achieved by allocating the available power to other subcarriers with less interference. Furthermore in the presence of co-channel interference, subcarrier 8 can be used to enhance the performance of user 2.

In case of unequal power initialization, the interference is not only influenced by the channel gain but also by the allocated power. The main difference is the increased power allocation at $u, k = 1, 8$ and decreased at $u, k = 1, 2$. Unlike in the case of equal power initialization, the power allocation depends on both the channel gain and the allocated power. Here $u, k = 1, 8$ with good channel gain and sufficient initial allocated power, is able to suppress the interference and produce better SINR.

Table 5.4 shows the comparison of power allocation pattern between $R_u = 2$ and $R_u = 15$. First of all it can be observed that at $R_u = 15$, more power is required initially to satisfy the feasibility condition as compared to $R_u = 2$. Increase in R_u increases the QoS demand per user. Therefore in order to satisfy the QoS constraints, more power is allocated to each subcarrier when $R_u = 15$.

Table 5.4: Comparison of power Allocation between $R_u = 2$ and $R_u = 15$ at $\theta = 1$.

u, k	Equal Power Initialization at Rate=2		Equal Power Initialization at Rate=15	
	Initial	Final	Initial	Final
1,1	0.5	0.44273	4.5	5.0317
1,2	0.5	0.16435	4.5	3.1785
1,3	0.5	0.00092	4.5	0.0028
1,4	0.5	0.00093	4.5	3.8113
1,5	0.5	0.24564	4.5	4.8369
1,6	0.5	0.09364	4.5	2.371
1,7	0.5	0.00093	4.5	4.3229
1,8	0.5	0.09749	4.5	2.3178
2,1	0.5	0.00074	4.5	0.0019
2,2	0.5	0.05501	4.5	3.3914
2,3	0.5	0.26284	4.5	4.5798
2,4	0.5	0.00074	4.5	3.5821
2,5	0.5	0.00070	4.5	0.0064
2,6	0.5	0.00359	4.5	2.759
2,7	0.5	0.31242	4.5	4.6857
2,8	0.5	0.18265	4.5	3.4947
3,1	0.5	0.00076	4.5	3.2804
3,2	0.5	0.00076	4.5	0.0075
3,3	0.5	0.02564	4.5	3.448
3,4	0.5	0.391	4.5	3.8088
3,5	0.5	0.35181	4.5	3.8588
3,6	0.5	0.00075	4.5	2.86
3,7	0.5	0.00076	4.5	0.0070
3,8	0.5	0.00200	4.5	2.3594

Furthermore, in the case of $R_u = 15$, higher number of subcarriers are utilized for transmission; even those with smaller channel gains. For example in case of $R_u = 2$, the performance enhancing subcarriers (high SINR subcarriers) of user 1 are $u, k = 1, 1$, $u, k = 1, 2$ and $u, k = 1, 5$ whereas in case of $R_u = 15$ almost all the subcarriers are used with some amount of power except $u, k = 1, 3$ i.e. the one with the lowest channel gain.

Table 5.5 shows the power allocation pattern at $R_u = 2$ and $\theta = 0$. Here the objective function only minimizes the SPV and not the sum power. The final allocated power corresponds to the minimum achieved SPV per user. The goal is to determine the optimal power distribution over N_F subcarriers of each user such that SPV can be reduced significantly. The power allocation is based on the expression

$$\sigma_P^2 = \frac{2}{N_F^2} \sum_{\substack{p,q=1 \\ q>p}}^{N_F} P_p P_q \tag{5.1}$$

where σ_P^2 is SPV and P_i is the power allocated to the i^{th} subcarrier. The derivation for (5.1) is shown in the Appendix 1. The SPV in (5.1) is the squared deviation of power from its mean, evaluated per user. The subscript u denoting user is omitted here for simplicity. The term σ_P^2 measures the spread of power distribution or in other words it measures the degree at which the powers at different subcarriers differ from each other. Decreasing the spread of power distribution decreases the SPV and consequently decreases the PAPR. The SPV and consequently PAPR can be minimized when all the power is allocated to the single subcarrier. It can be seen that the algorithm increases

the power of the single subcarrier with the highest initial power while reduces the power of all the other subcarriers. It can be observed that $u, k = 1, 7$, $u, k = 2, 8$ and $u, k = 3, 2$ have the highest initial power. Therefore, the final allocated power at these subcarriers of respective users are highly increased.

Table 5.5: Power Allocation at at $R_u = 2$, $\theta = 0$.

u, k	Power Initialization $P_{u,k}$	
	Initial	Final
1,1	0.0001	0.0001
1,2	0.0001	0.0001
1,3	0.0001	0.0001
1,4	0.0001	0.0001
1,5	0.0001	0.0001
1,6	0.0001	0.0001
1,7	10000	5.0667
1,8	1.0001	0.0003
2,1	0.0001	0.0001
2,2	0.0001	0.0001
2,3	0.0001	0.0001
2,4	0.0001	0.0001
2,5	0.0001	0.0001
2,6	0.0001	0.0001
2,7	1.0001	0.0003
2,8	10000	4.8366
3,1	0.0001	0.0001
3,2	10000	5.1873
3,3	0.0001	0.0001
3,4	1.0001	0.0003
3,5	0.0001	0.0001
3,6	0.0001	0.0001
3,7	0.0001	0.0001
3,8	0.0001	0.0001

Table 5.6 shows the power allocation pattern at $R_u = 2$ and $\theta = 0.01$ i.e. stress for minimization is 0.99 and 0.01 for SPV and sum power respectively. In this case, the algorithm minimizes both the sum power and SPV by taking the channel gain into account. The combined affect of both the constraints can be observed from the data. Here $u, k = 1, 1$ is prioritized due to the high channel gain but in presence of SPV constraint, the power minimization is not much effective as it can be seen that the final allocated power is higher than the initial power. This is due to the SPV constraint trying to increase the power of single subcarrier with highest power; here in this case subcarrier 1. However, the SPV constraint cannot completely minimize the spread by reducing power of other subcarriers as in case of $\theta = 0$. It can be seen that the SINR constraint does not allow the powers at $u, k = 1, 5$ and $u, k = 1, 8$ to be completely minimized due to the high channel gain.

CCDF plots for PAPR distribution using gaussian symbols at different θ are analyzed in Fig. 5.1, Fig. 5.2, Fig. 5.3 and Fig. 5.4 for $R_u = 2$, $R_u = 3$, $R_u = 4$ and $R_u = 16$ respectively. The contribution of SPV constraint in PAPR reduction can be seen at $\theta = 0$. But as θ increases, the SINR constraint is much more dominant compared to SPV constraint, hence it is difficult to realize significant PAPR reduction at higher θ. However, the affect of SPV constraint can be observed at range of θ close to 0 i.e.

when more weight is assigned to SPV in the objective.

It can also be seen that at higher rate constraint the power allocation algorithm does not allocate all the power to the single subcarrier which is essential in order to minimize the SPV but instead distributes among multiple subcarriers. This is due to the rate constraint expression $log_2(1 + \gamma)$. This causes rate to increase linearly at low rate and logarithmically at high rate. Satisfying the high rate requirement by using only one subcarrier leads to a very high power value that may cause numerical problems. Therefore, numerical results may differ in a way such that the high rate constraint tends to distribute the power to several subcarriers. The numerical results may be affected by the computing environment such as hardware capability, operating system and modeling language. It may cause to produce inaccurate results when dealing with high values close to infinity or when there is very large amount of power difference between subcarriers. Moreover, at higher rates number of possible PAPR distributions seems to decrease as the CCDF curves align with each other.

Table 5.6: Power Allocation at $R_u = 2$, $\theta = 0.01$.

u, k	Unequal Power Initialization	
	Initial	Final
1,1	0.12814	0.81286
1,2	0.01448	0.00193
1,3	0.33829	0.00073
1,4	0.19869	0.00073
1,5	0.51061	0.12057
1,6	0.91122	0.02277
1,7	0.69697	0.00073
1,8	0.71098	0.16045
2,1	0.65655	0.00054
2,2	0.4761	0.09271
2,3	0.27539	0.15727
2,4	1.1469	0.00056
2,5	2.3014	0.00065
2,6	0.19508	0.00054
2,7	1.2183	0.65791
2,8	0.22136	0.00349
3,1	1.0074	0.00048
3,2	0.51458	0.00067
3,3	1.1027	0.00397
3,4	0.37152	0.54051
3,5	1.1066	0.24855
3,6	0.39917	0.00048
3,7	0.31508	0.00048
3,8	0.72451	0.00066

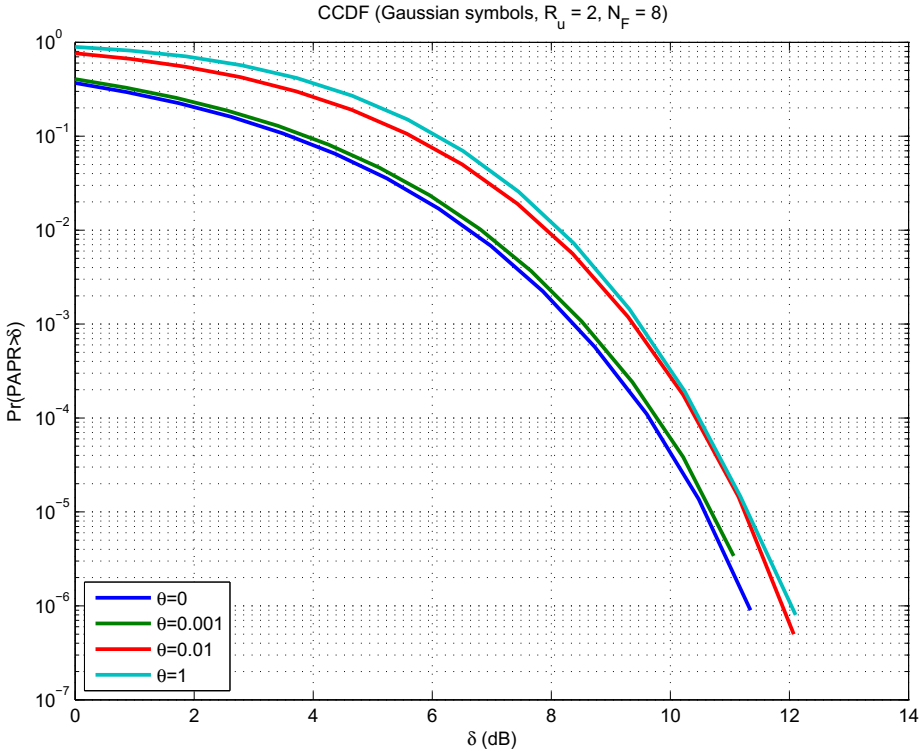

Figure 5.1: CCDF plot for $R_u = 2$.

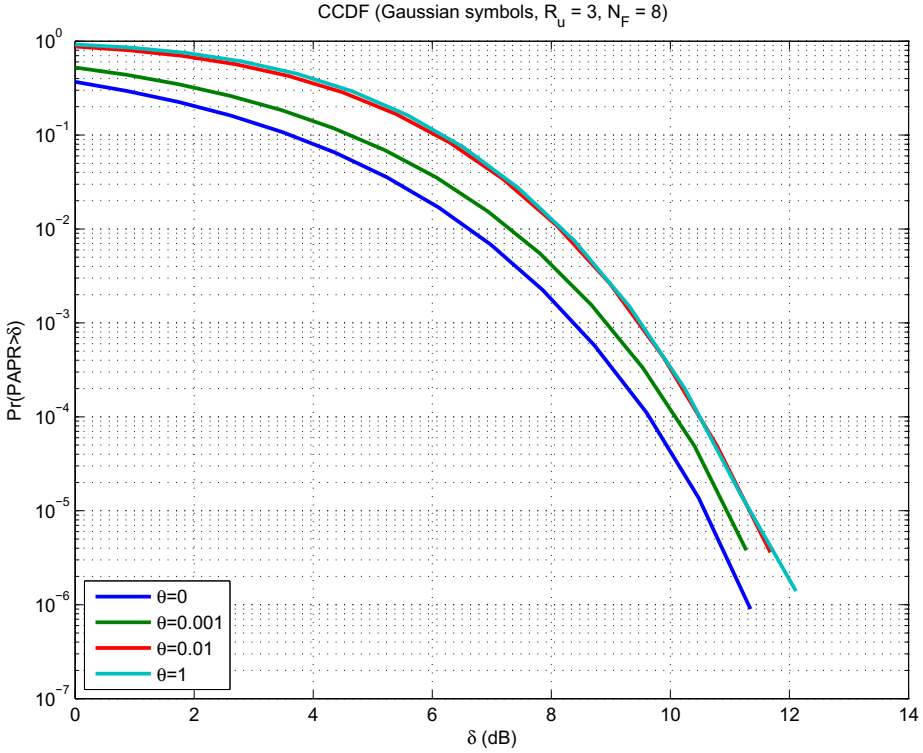

Figure 5.2: CCDF plot for $R_u = 3$.

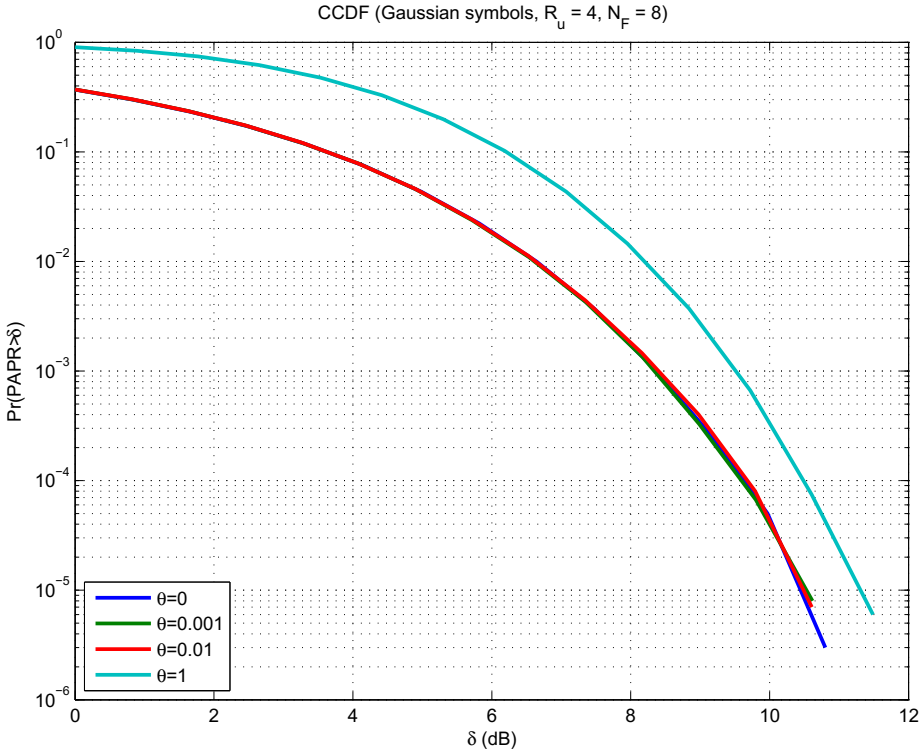

Figure 5.3: CCDF plot for $R_u = 3$.

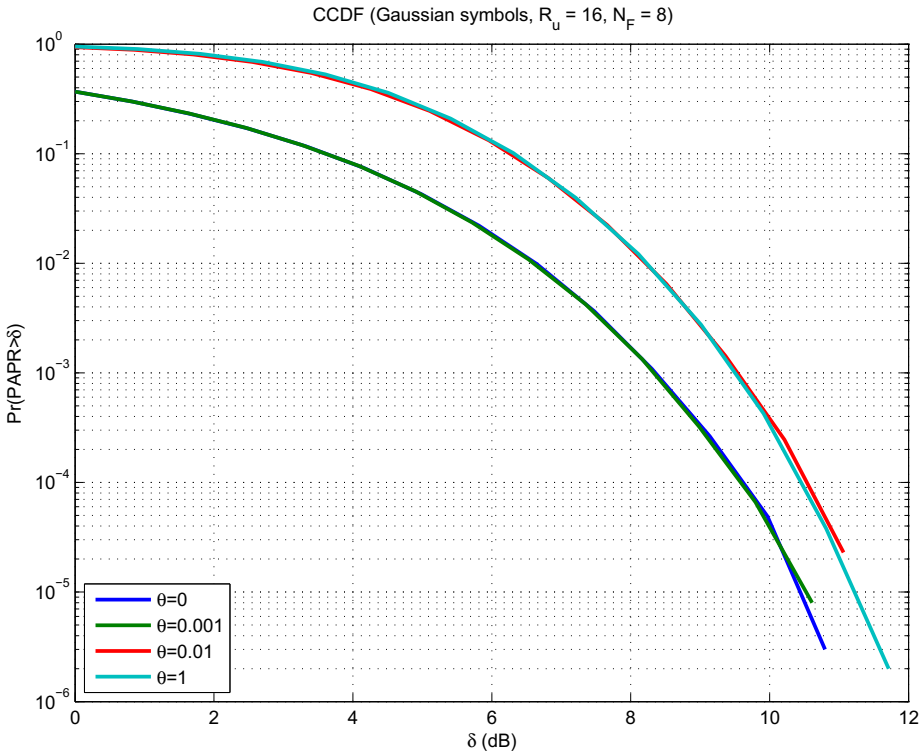

Figure 5.4: CCDF plot for $R_u = 3$.

6. DISCUSSION

This thesis aims to develop an algorithm for optimal power allocation in MU SIMO-OFDMA system in UL by taking PAPR under consideration. The main objective of the power allocation scheme is to increase the power efficiency of battery operated devices in UL and reduce co-channel interference in OFDMA system by minimizing PAPR and power consumption while maintaining certain user specified QoS.

Based on statistical property of PAPR distribution as discussed in Chapter 2, the intuitive approach of minimizing the SPV is preferred to reduce the variability between the powers at different subcarriers. The MU SIMO-OFDMA UL system model used for implementing the algorithm is explained with stepwise mathematical description in Chapter 3. The problem formulation for proposed algorithms are shown in Chapter 4. The power to be allocated to the subcarriers of each user is calculated in a centralized manner by the BS with knowledge of entire channel. The power allocation problem is solved using convex optimization. The joint optimization algorithm adjusts the transmit power and receive beamformers alternately, until convergence. The presence of co-channel interference in MU OFDMA UL system results in non-convex interference coupled SINR function with respect to power. The convex transformation is achieved by employing COV to transform the power into log-domain. Furthermore, SCA is employed to approximate the non-convex SINR constraint as convex. The point of convergence is such that sum power and SPV are minimized and certain QoS is satisfied. Due to the conflicting nature of mathematical relation between power and SPV, the simultaneous minimization of both parameters requires the multi objective formulation of convex optimization problem using relaxation technique. Furthermore, several Pareto solutions are determined based on the minimization priority among either power or SPV. SPV constraint aims to allocate all the power to single subcarrier; consequently reducing the PAPR.

The power allocation algorithm is facilitated by scheduling flexibility of OFDMA system with further enhancement in resource components by SIMO technology. The algorithm attempts to reduce the PAPR during the power allocation stage, performed on frequency domain samples of OFDM symbol. The opportunistic behaviour in scheduling based on channel gains results from competitive nature of users due to interference imposed to each other in co-channel. The competition among the users can be eliminated by orthogonalizing the users such that only single user is transmitting in each channel, thus eliminating co-channel interference. However, it relates to trade-off between degree of resource utilization and reception quality. Therefore based on the channel state of users, the scheduling can exploit either multiuser diversity or frequency diversity for best possible resource utilization. Despite all the benefits, the synchronization issue imposes threat on distortion free reception of orthogonal subcarriers.

The numerical results for the derived algorithms are presented in Chapter 5. The effect of individual constraint, namely rate and SPV on the resulting power allocation pattern is analyzed followed by the combined effect of the both constraints. It has been shown using gaussian transmitted symbols that reducing the SPV reduces the PAPR. However, the SPV constraint is seen to be effective when it has highest minimizing priority among the objective function. As the priority deviates towards sum power minimization, the SINR constraint highly dominates the SPV constraint. The PAPR distribution is inspected varying the strength of SPV in the objective and also at various QoS requirements.

The PAPR causes major system degradation in OFDMA UL system causing signal distortion at the transmitter due to erroneous behavior in the radio frequency (RF) circuitry. Signal processing at high PAPR requires expensive HPA and mainly degrades the power efficiency. Although the advanced communication standards such as LTE employs SC-FDMA as a variant of OFDMA for UL transmission due to reduced PAPR, the SC-FDMA lacks various advantageous scheduling flexibility offered by OFDMA. On the other hand, minimizing power consumption is equally critical issue with respect to interference management and prolong battery life of wireless devices. The issue raised in this thesis can be further examined to procure better trade-off between the minimization of both PAPR and power consumption. Furthermore scheduling features of adaptive OFDMA can be exploited to maintain the required QoS by varying the modulation and coding at individual subcarrier, of course at the cost of increased complexity. The power allocation can be performed in a distributive manner where each MT computes its own power, oblivious to the channel state of any other MTs in the system. By sufficiently minimizing the PAPR, OFDMA can thrive as an efficient multiple access technique for future communication standards.

BIBLIOGRAPHY

[1] Nee R.v. & Prasad R. (2000) OFDM for wireless multimedia communications. Artech House, Inc.

[2] Mosier R. & Clabaugh R. (1958) Kineplex, a bandwidth-efficient binary transmission system. American Institute of Electrical Engineers, Part I: Communication and Electronics, Transactions of the 76, pp. 723–728.

[3] Chang R.W. (1966) Synthesis of band-limited orthogonal signals for multichannel data transmission. Bell System Technical Journal 45, pp. 1775–1796.

[4] Saltzberg B. (1967) Performance of an efficient parallel data transmission system. Communication Technology, IEEE Transactions on 15, pp. 805–811.

[5] Group I..W. et al. (2005) Ieee standard for local and metropolitan area networks. part 16: Air interface for fixed broadband wireless access systems. amendment 2: Physical and medium access control layer for combined fixed and mobile operation in licensed bands. IEEE Std 802.

[6] Bacioccola A., Cicconetti C., Eklund C., Lenzini L., Li Z. & Mingozzi E. (2010) Ieee 802.16: History, status and future trends. Computer Communications 33, pp. 113–123.

[7] 3rd Generation Partnership Project (3GPP); Technical Specification Group Radio Access Network 3. Technical report.

[8] Sampath H., Talwar S., Tellado J., Erceg V. & Paulraj A. (2002) A fourth-generation mimo-ofdm broadband wireless system: design, performance, and field trial results. Communications Magazine, IEEE 40, pp. 143–149.

[9] Ganesan A. & Sayeed A.M. (2003) A virtual input-output framework for transceiver analysis and design for multipath fading channels. Communications, IEEE Transactions on 51, pp. 1149–1161.

[10] Bolcskei H., Gesbert D. & Paulraj A.J. (2002) On the capacity of ofdm-based spatial multiplexing systems. Communications, IEEE Transactions on 50, pp. 225–234.

[11] Han S.H. & Lee J.H. (2005) An overview of peak-to-average power ratio reduction techniques for multicarrier transmission. Wireless Communications, IEEE 12, pp. 56–65.

[12] Lee Y.L., You Y.H., Jeon W.G., Paik J.H. & Song H.K. (2003) Peak-to-average power ratio in mimo-ofdm systems using selective mapping. Communications Letters, IEEE 7, pp. 575–577.

[13] Moon J.H., You Y.H., Jeon W.G., Kwon K.W. & Song H.K. (2003) Peak-to-average power control for multiple-antenna hiperlan/2 and ieee802. 11a systems. Consumer Electronics, IEEE Transactions on 49, pp. 1078–1083.

[14] Karjalainen J., Codreanu M., Tolli A., Juntti M. & Matsumoto T. (2011) Exit chart-based power allocation for iterative frequency domain mimo detector. Signal Processing, IEEE Transactions on 59, pp. 1624–1641.

[15] Tervo V., Tolli A., Karjalainen J. & Matsumoto T. (2012) On convergence constraint precoder design for iterative frequency domain multiuser siso detector. In: *Signals, Systems and Computers (ASILOMAR), 2012 Conference Record of the Forty Sixth Asilomar Conference on*, IEEE, pp. 473–477.

[16] Tervo V., Tölli A., Karjalainen J. & Matsumoto T. (2013) Papr constrained power allocation for iterative frequency domain multiuser simo detector. arXiv preprint arXiv:1311.5376 .

[17] Weinstein S.B. & Ebert P.M. (October 1971) Data transmission by frequency division multiplexing using the discrete Fourier transform. IEEE Transactions on Communication Technology 19, pp. 628–634.

[18] Hanzo L., Webb W. & Keller T. (April 2000) Single- and Multi-carrier Quadrature Amplitude Modulation: Principles and Applications for Personal Communications, WATM and Broadcasting: 2nd. IEEE Press-John Wiley.

[19] Speth M., Classen F. & Meyr H. (May 1997) Frame synchronization of ofdm systems in frequency selective fading channels. In: *Vehicular Technology Conference, 1997, IEEE 47th*, volume 3, pp. 1807–1811 vol.3.

[20] Ochiai H. (1997) Block coding scheme based on complementary sequences for multicarrier signals. IEICE TRANSACTIONS on Fundamentals of Electronics, Communications and Computer Sciences 80, pp. 2136–2143.

[21] Rumney M. et al. (2013) LTE and the evolution to 4G wireless: Design and measurement challenges. John Wiley & Sons.

[22] Annis C. (2004), Central limit theorem.

[23] Ochiai H. & Imai H. (2001) On the distribution of the peak-to-average power ratio in ofdm signals. Communications, IEEE Transactions on 49, pp. 282–289.

[24] Gregorio F. & Laakso T. (2005) The performance of ofdm-sdma systems with power amplifier non-linearitiesâĂŰ. In: *Proceeding of the 2005 Finnish Signal Processing Symposium-FINSIG*, Citeseer, volume 5.

[25] Li X. & Cimini L.J. (1997) Effects of clipping and filtering on the performance of ofdm. In: *Vehicular Technology Conference, 1997, IEEE 47th*, IEEE, volume 3, pp. 1634–1638.

[26] De Wild A. (1997) The peak-to-average power ratio of ofdm. Ph.D. thesis, M. Sc. Thesis, Delft University of Technology, Delft.

[27] Nikookar H. & Lidsheim K.S. (2002) Random phase updating algorithm for ofdm transmission with low papr. Broadcasting, IEEE Transactions on 48, pp. 123–128.

[28] Huang X., Lu J., Zheng J., Letaief K.B. & Gu J. (2004) Companding transform for reduction in peak-to-average power ratio of ofdm signals. Wireless Communications, IEEE Transactions on 3, pp. 2030–2039.

[29] Golay M.J. (1961) Complementary series. Information Theory, IRE Transactions on 7, pp. 82–87.

[30] Davis J.A. & Jedwab J. (1999) Peak-to-mean power control in ofdm, golay complementary sequences, and reed-muller codes. Information Theory, IEEE Transactions on 45, pp. 2397–2417.

[31] Irukulapati N., Chakka V. & Jain A. (2009) Slm based papr reduction of ofdm signal using new phase sequence. Electronics letters 45, pp. 1231–1232.

[32] Müller S.H. & Huber J.B. (1997) Ofdm with reduced peak-to-average power ratio by optimum combination of partial transmit sequences. Electronics letters 33, pp. 368–369.

[33] Coulson A. (Dec 2001) Maximum likelihood synchronization for ofdm using a pilot symbol: algorithms. Selected Areas in Communications, IEEE Journal on 19, pp. 2486–2494.

[34] Goldsmith A.J. & Chua S.G. (1997) Variable-rate variable-power mqam for fading channels. Communications, IEEE Transactions on 45, pp. 1218–1230.

[35] Tervo V., Tölli A., Karjalainen J. & Matsumoto T. (2013) Convergence constrained multiuser transmitter-receiver optimization in single carrier fdma. IEEE Transaction Signal Processing, .

[36] Grandhi S., Vijayan R., Goodman D. & Zander J. (November 1993) Centralized power control in cellular radio systems 42.

[37] Zander J. (Feb 1992) Performance of optimum transmitter power control in cellular radio systems. Vehicular Technology, IEEE Transactions on 41, pp. 57–62.

[38] Gantmacher F.R. (199) The theory of matrices 2.

[39] Sari H. & Karam G. (1998) Orthogonal frequency-division multiple access and its application to catv networks. European transactions on telecommunications 9, pp. 507–516.

[40] Bolton W., Xiao Y. & Guizani M. (2007) Ieee 802.20: mobile broadband wireless access. Wireless Communications, IEEE 14, pp. 84–95.

[41] ETSI (2000) Broadband radio access networks (BRAN); HIPERLAN type 2; system overview, ts 101 683 v1.1.1 (2000-02). Technical report, European Telecommunications Standards Institute (ETSI).

[42] DVB-RCT E. (2001) Interaction channel for digital terrestrial television (rct) incorporating multiple access ofdm. Sophia Antipolis, France .

[43] Wei L. & Schlegel C. (1995) Synchronization requirements for multi-user ofdm on satellite mobile and two-path rayleigh fading channels. Communications, IEEE Transactions on 43, pp. 887–895.

[44] Group I..W. et al. (2004) Ieee standard for local and metropolitan area networks, part 16: Air interface for fixed broadband wireless access systems. IEEE Std 802, pp. 16–2004.

[45] Myung H.G., Lim J. & Goodman D. (2006) Peak-to-average power ratio of single carrier fdma signals with pulse shaping. In: *Personal, Indoor and Mobile Radio Communications, 2006 IEEE 17th International Symposium on*, IEEE, pp. 1–5.

[46] Katz M.D. & Fitzek F.H. (2009) WiMAX Evolution. Wiley Online Library.

[47] Goldsmith A., Jafar S., Jindal N. & Vishwanath S. (June 2003) Capacity limits of mimo channels. Selected Areas in Communications, IEEE Journal on 21, pp. 684–702.

[48] Boyd S. & Vandenberghe L. (2004) Convex Optimization. Cambridge University Press.

[49] Yates R.D. (September 1995) A framework for uplink power control in cellular radio 13, pp. 1341–1347.

[50] Boche H. & Naik S. (Nov 2009) Impact of interference coupling - loss of convexity. In: *Global Telecommunications Conference, 2009. GLOBECOM 2009. IEEE*, pp. 1–6.

[51] Boche H. & Stanczak S. (Sept 2003) Log-convexity of minimal feasible total power in cdma channels. In: *Personal, Indoor and Mobile Radio Communications, 2003. PIMRC 2003. 14th IEEE Proceedings on*, volume 2, pp. 1456–1460 vol.2.

[52] Sung C.W. (June 2002) Log-convexity property of the feasible sir region in power-controlled cellular systems. Communications Letters, IEEE 6, pp. 248–249.

[53] Kaleva J., Tolli A. & Juntti M. (Dec 2012) Weighted sum rate maximization for interfering broadcast channel via successive convex approximation. In: *Global Communications Conference (GLOBECOM), 2012 IEEE*, pp. 3838–3843.

Appendix 1: Signal power variance derivation

The power variance of the transmitted OFDM signal is studied. Subscript u is omitted for simplicity.

Let

$$G = F^{-1}\sqrt{P}$$

where

$F \in \mathbb{C}^{N_F \times N_F}$ is the DFT matrix whose element is given by

$$f_{k,m} = \frac{1}{\sqrt{N_F}} e^{(i2\pi(m-1)(k-1)/N_F)}, \;\; k, m = 1, 2, \cdots, N_F$$

$P \in \mathbb{C}^{N_F \times N_F}$ is the diagonal power allocation matrix.

Therefore each element of G matrix can be represented as

$$g_{k,m} = \frac{1}{\sqrt{N_F}} e^{(i2\pi(m-1)(k-1)/N_F)} \sqrt{P_m}, \qquad k, m = 1, 2, \cdots, N_F$$
$$|g_{k,m}|^2 = \frac{P_m}{N_F}, \qquad (FF^{-1} = I)$$

The transmitted time domain passband OFDM signal can be written as

$$s_k = \textstyle\sum_{m=1}^{N_F} g_{k,m} b_m \;\; k = 1, 2, \cdots, N_F$$

where b is the frequency domain baseband signal. The k^{th} subcarrier with the highest power among the N_F subcarriers of user u is given by

$$\max(|s_u|^2) = \max_{k \in [1, N_F]} (|s_k|^2) = \max(|s_1|^2, |s_2|^2, \cdots, |s_{N_F}|^2) \tag{A1.1}$$

The following assumptions are considered

$$\begin{aligned} \mathbb{E}\{|b_m|\} &= 1 \\ \mathbb{E}\{|b_m b_m^*|\} &= 1 \\ \mathbb{E}\{|b_m b_n^*|\} &= 0, \qquad \forall m \neq n \end{aligned}$$

The *Average Power* μ_P of the transmitted OFDM signal can be calculated as

$$\begin{aligned} \mu_P = avg[|s_k|^2] &= \frac{1}{N_F} \sum_{k=1}^{N_F} \mathbb{E}\{|s_k|^2\} \\ &= \frac{1}{N_F} \sum_{k=1}^{N_F} \mathbb{E}\{|\sum_{m=1}^{N_F} g_{k,m} b_m|^2\} \\ &= \frac{1}{N_F} \sum_{k=1}^{N_F} \mathbb{E}\{(\sum_{m=1}^{N_F} g_{k,m} b_m)(\sum_{m=1}^{N_F} g_{k,m}^* b_m^*)\} \end{aligned}$$

$$= \frac{1}{N_F}\sum_{k=1}^{N_F}\mathbb{E}\{\sum_{m=1}^{N_F}|g_{k,m}|^2|b_m|^2 + \sum_{\substack{p,q=1\\p\neq q}}^{N_F}(g_{k,p}g_{k,q}^*b_pb_q^*)\}$$

$$= \frac{1}{N_F}\sum_{k=1}^{N_F}\sum_{m=1}^{N_F}|g_{k,m}|^2$$

$$= \frac{1}{N_F}\sum_{m=1}^{N_F}N_F\frac{P_m}{N_F}$$

$$\therefore \mu_P = \frac{1}{N_F}\sum_{m=1}^{N_F}P_m \tag{A1.2}$$

OFDM Power Variance

Variance is measured as the expectation of the squared deviation the variable's value from the variable's expected value. From the definition the power variance of the OFDM signal can be represented as

$$\sigma_P^2 = \frac{1}{N_F}\sum_{k=1}^{N_F}\mathbb{E}\{|s_k|^2-\mu_P\}^2$$

$$= \frac{1}{N_F}\sum_{k=1}^{N_F}\mathbb{E}\{|s_k|^4\}-\mu_P^2$$

$$= \frac{1}{N_F}\sum_{k=1}^{N_F}\mathbb{E}\{(\sum_{m=1}^{N_F}g_{k,m}b_m)(\sum_{m=1}^{N_F}g_{k,m}^*b_m^*)\}^2-\mu_P^2$$

$$= \frac{1}{N_F}\sum_{k=1}^{N_F}\mathbb{E}\{\sum_{m=1}^{N_F}(|g_{k,m}|^2|b_mb_m^*|)+\sum_{\substack{p,q=1\\p\neq q}}^{N_F}(g_{k,p}g_{k,q}^*b_pb_q^*)\}^2-\mu_P^2$$

$$= \frac{1}{N_F}\sum_{k=1}^{N_F}\mathbb{E}\{\sum_{m=1}^{N_F}(|g_{k,m}|^2)+\sum_{\substack{p,q=1\\p\neq q}}^{N_F}(g_{k,p}g_{k,q}^*b_pb_q^*)\}^2-\mu_P^2$$

$$= \frac{1}{N_F}\sum_{k=1}^{N_F}\mathbb{E}\{(\sum_{m=1}^{N_F}|g_{k,m}|^2)^2+2\sum_{m=1}^{N_F}|g_{k,m}|^2\sum_{\substack{p,q=1\\p\neq q}}^{N_F}g_{k,p}g_{k,q}^*b_pb_q^*+(\sum_{\substack{p,q=1\\p\neq q}}^{N_F}g_{k,p}g_{k,q}^*b_pb_q^*)^2\}-\mu_P^2$$

$$= \frac{1}{N_F}\sum_{k=1}^{N_F}[(\sum_{m=1}^{N_F}|g_{k,m}|^2)^2+\mathbb{E}\{\sum_{\substack{p,q=1\\p\neq q}}^{N_F}|g_{k,p}|^2|g_{k,q}^*|^2|b_pb_p^*||b_qb_q^*|\}^2]-\mu_P^2$$

$$= \frac{1}{N_F}\sum_{k=1}^{N_F}[(\sum_{m=1}^{N_F}|g_{k,m}|^2)^2+\sum_{\substack{p,q=1\\p\neq q}}^{N_F}|g_{k,p}|^2|g_{k,q}^*|^2]-\mu_P^2$$

$$= \frac{1}{N_F}\sum_{k=1}^{N_F}[(\sum_{m=1}^{N_F}|g_{k,m}|^2)^2 + \sum_{m=1}^{N_F}|g_{k,m}|^4 + \sum_{\substack{p,q=1 \\ p\neq q}}^{N_F}|g_{k,p}|^2|g_{k,q}^*|^2 - \sum_{m=1}^{N_F}|g_{k,m}|^4] - \mu_P^2$$

$$\therefore \sigma_P^2 = \underbrace{\frac{1}{N_F}\sum_{k=1}^{N_F}2(\sum_{m=1}^{N_F}|g_{k,m}|^2)^2} - \underbrace{\frac{1}{N_F}\sum_{k=1}^{N_F}\sum_{m=1}^{N_F}|g_{k,m}|^4} - \mu_P^2 \tag{A1.3}$$

Each term in the equation (A1.3) is evaluated separately.

- First Term

$$\begin{aligned}
&= \frac{1}{N_F}\sum_{k=1}^{N_F}[2\sum_{m=1}^{N_F}|g_{k,m}|^2]^2 \\
&= \frac{2}{N_F}\sum_{k=1}^{N_F}[\sum_{m=1}^{N_F}|g_{k,m}g_{k,m}^*|]^2 \\
&= \frac{2}{N_F}\sum_{k=1}^{N_F}[\sum_{m=1}^{N_F}frac1N_FP_m]^2 \\
&= \frac{2}{N_F}\sum_{k=1}^{N_F}\mu_P^2 \\
&= \frac{2}{N_F}N_F\mu_P^2 \\
&= 2\mu^2
\end{aligned}$$

- Second Term

$$\begin{aligned}
&= \frac{1}{N_F}\sum_{k=1}^{N_F}\sum_{m=1}^{N_F}|g_{k,m}|^4 \\
&= \frac{1}{N_F}\sum_{k=1}^{N_F}\sum_{m=1}^{N_F}|g_{k,m}g_{k,m}^*|^2 \\
&= \frac{1}{N_F}\sum_{k=1}^{N_F}\sum_{m=1}^{N_F}[\frac{1}{N_F}P_m]^2 \\
&= \frac{1}{N_F^3}\sum_{k=1}^{N_F}N_FP_m^2 \\
&= \frac{1}{N_F^2}\sum_{k=1}^{N_F}P_m^2
\end{aligned}$$

Substituting the result back to equation (A1.3)

$$\begin{aligned}
\sigma_P^2 =& 2\mu^2 - \frac{1}{N_F^2}\sum_{m=1}^{N_F} P_m^2 - \mu_P^2 \\
=& \mu^2 - \frac{1}{N_F^2}\sum_{m=1}^{N_F} P_m^2 \\
=& [\frac{1}{N_F}\sum_{m=1}^{N_F} P_m]^2 - \frac{1}{N_F^2}\sum_{m=1}^{N_F} P_m^2 \\
=& \frac{1}{N_F^2}[(\sum_{m=1}^{N_F} P_m)^2 - \sum_{m=1}^{N_F} P_m^2] \\
=& \frac{1}{N_F^2}[\sum_{m=1}^{N_F} P_m^2 + 2\sum_{\substack{p,q=1 \\ q>p}}^{N_F} P_p P_q - \sum_{m=1}^{N_F} P_m^2]
\end{aligned}$$

$$\sigma_P^2 = \frac{2}{N_F^2}\sum_{\substack{p,q=1 \\ q>p}}^{N_F} P_p P_q \qquad \text{(A1.4)}$$

Appendix 2: Static channel impulse response

The fixed channel gain $h^r_{u,l}$ for every user-receive antenna pair used in simulation.

(a) User 1.

	$h^r_{1,1}$	$h^r_{1,2}$	$h^r_{1,3}$
$r = 1$	-0.1511+0.1021i	0.3856-0.1668i	0.18-0.1478i
$r = 2$	0.1227+0.02427i	0.1318-0.3177i	0.2657+0.1037i
$r = 3$	-0.08973-0.1344i	0.1329-0.4135i	0.03337-0.3542i
$r = 4$	0.4697+0.1162i	-0.07976-0.08575i	0.4545-0.04908i

(b) User 2.

	$h^r_{2,1}$	$h^r_{2,2}$	$h^r_{2,3}$
$r = 1$	0.1581-0.3548i	-0.09385+0.1167i	0.2231+0.3424i
$r = 2$	-0.02595+0.4266i	-0.02014+0.2142i	0.1928-0.4895i
$r = 3$	0.08744-0.02757i	0.5594-0.2721i	0.3745-0.0416i
$r = 4$	0.2585+0.289i	-0.1117+0.2964i	0.124-0.1537i

(c) User 3.

	$h^r_{3,1}$	$h^r_{3,2}$	$h^r_{3,3}$
$r = 1$	-0.5811+0.0369i	0.4626+0.05768i	-0.365-0.1228i
$r = 2$	-0.2009-0.2004i	0.3315-0.02789i	0.4392-0.3015i
$r = 3$	0.1206+0.06577i	0.1171-0.3039i	0.03159-0.01325i
$r = 4$	0.06076+0.1407i	0.01952+0.01357i	-0.3644-0.04942i